NACA [redacted]

RESEARCH MEMORANDUM

COMPILATION AND ANALYSIS OF U. S. TURBOJET AND RAM-JET ENGINE CHARACTERISTICS

By Richard S. Cesaro and Curtis L. Walker

NATIONAL ADVISORY COMMITTEE
FOR AERONAUTICS
WASHINGTON
November 27, 1956

Engines, Turbojet 3.1.3

Nuclear Energy Systems 3.1.10

Engine Types, Comparison 3.1.12

Fuels - Relation to Engine Performance 3.4.3

Cesaro, Richard S., and Walker, Curtis L.

COMPILATION AND ANALYSIS OF U. S. TURBOJET AND RAM-JET ENGINE CHARACTERISTICS

Abstract

A compilation and analysis of sea-level static and flight performance data on existing and designed U. S. axial-flow turbojet and ram-jet engines is presented. Factors relating to engine size, performance, and weight are examined for trends, and actual and theoretical performances are compared.

NACA RM S56K19

NATIONAL ADVISORY COMMITTEE FOR AERONAUTICS

RESEARCH MEMORANDUM

COMPILATION AND ANALYSIS OF U. S. TURBOJET AND RAM-JET ENGINE CHARACTERISTICS

By Richard S. Cesaro and Curtis L. Walker

SUMMARY

A compilation of sea-level static and flight-performance data for existing and designed U. S. axial-flow turbojet and ram-jet engines is presented. Factors relating to engine size, performance, and weight are examined for trends and actual and theoretical performances are compared.

INTRODUCTION

As a result of intense research and development, gas turbine engine performance has advanced at a tremendous rate. Accompanying this progress, a large number of engine designs have emerged to meet the many applications. The large number of engines with various levels of performance made desirable the collection and analysis of characteristic data on the various engines. Such a survey was made and reported approximately 5 years ago in reference 1. Because of continued advances and increases in number of proposed engines, the present report, prepared at the request of the Air Force and the Navy Bureau of Aeronautics, essentially brings up to date the data presented in reference 1, and in addition, includes flight performance data on both ram-jet and turbojet engines.

The primary purpose of this report is to present an over-all picture of the current U. S. engine capability and the future growth potential as reflected in advanced engine designs. The data as presented also provide information that could assist in aircraft design analysis, indicate certain operational requirements for research test facilities, and point out areas in the engine-development program possibly requiring further emphasis.

The figures presented are arranged to meet the following three main objectives:

(1) To indicate the engines available in any time period;

(2) To present basic engine variables that reflect technical advances, if any;

(3) To present changes brought about in engine weight reductions caused by improvements in mechanical design or material selections.

For existing engines, the most recent operational data available are used. For design engines, the data are based on the performance specifications of the manufacturer. Since these specifications are changed during the production and design of the engines, discrepancies may exist between the data presented herein and other tabulations of this information. These differences will not be sufficient to affect the general trends presented. The engines presented in this report have completed or are estimated to complete their 150 hour test in the period from 1950 to 1960. Data presented herein have been compiled with the cooperation and assistance of the Department of Defense, the United States Air Force, the Navy Bureau of Aeronautics, and the aircraft engine industry.

DISCUSSION

Presentation of Data

Within the time period covered in this report, engine performance and size selections vary both as a result of technical advances and in order to meet aircraft and missile operational requirements. In order to illustrate these variations, figures are presented of engine variables, such as thrust and airflow for sea-level static conditions plotted against the completion time for the engine's 150 hour test. In each case the time used in plotting is the date the engine actually passed the 150 hour test or the estimated date the engine will pass the 150 hour test.

Fundamental thermodynamic arrangements can be made of engine variables to reveal technical advances that are designed into turbojet or ram-jet engines. For example, comparisons of actual engine performance with theoretical cycle calculations involving pressure ratio and turbine inlet temperature can indicate technical advances made in component efficiencies and cycle operating levels. Several figures are presented herein arranged to indicate these kinds of technical advances and are discussed from this point of view.

A similar comparison with theoretical calculations cannot be made for engine weight. Engine weight will reflect the ingenuity of mechanical designers and the development of materials for the engine. The weight data that are presented are intended to indicate general levels of engine and component weights expected to be achieved in various engine designs.

The engines presented herein are grouped in three general classes. They are as follows: (1) Design engines (data points are indicated by a circle); (2) development engines (data points are indicated by a square); (3) production engines (data points are indicated by a diamond). Engines with afterburners are indicated in the figures by tailed test-point symbols. Other symbols used on the figures are defined in the appendix; symbols used in the text are defined where used.

Information on some of the design engines is incomplete as far as detailed performance data are concerned. Theoretical performance curves determined from engine-cycle analysis are shown in some of the principal plots. Assumptions for theoretical curves are given in the appendix.

The performance data for an engine in the design stage do not change appreciably as the engine goes through the development and production stages. During this time basic components of the engine can and do change in order that its final performance may be in general agreement with the original design estimate. Performance data contained herein do not include the effect of several important design details and operating limits associated with individual engine designs. For example, engines designed for supersonic flight at sea level require strengthening of engine structure over that required for subsonic flight. On a weight basis, supersonic engines may show up at a disadvantage when compared with a subsonic engine. Further, most of the results presented are for sea-level static conditions and, as such, may not truly reflect the over-all utility or value of specific engines. However, certain data are presented under flight conditions so that some evaluation can be made of certain engine-design approaches. Although a comparison of design approaches is valid, the reader is cautioned against making specific engine comparisons indicating one engine to be superior to another.

Sea-Level Static Performance

Thrust. - Turbojet engine nonafterburning static sea-level thrust is plotted against completion of the 150 hour engine test in figure 1(a). The broken curve is from reference 1 and represents the same relation of thrust with time as predicted from data available in 1951. The solid lines, based on current data, represent the upper boundary of the engine size selections available in any time period. An approximate linear relation is indicated in this upper boundary line with sea-level static thrusts being increased from 10,000 pounds in 1950 to over 35,000 pounds in 1960. The shift in position from the broken line to the solid line indicates an increase of $1\frac{1}{2}$ to 2 years from the original estimates of time needed from design to completion of the 150 hour tests (ref. 1). It now takes between $4\frac{1}{2}$ to $5\frac{1}{2}$ years to bring an engine from design to

[redacted]

completion of its 150 hour test. Another important deviation from data presented in reference 1 is that at any time period a considerable range of engine thrust sizes is now available. In 1957, for example, the thrust range includes engines from 2,000 to 20,000 pounds thrust. In contrast, the data in reference 1 indicated no spread in thrust for engines available at a given time. Although a large number of engines are shown in the development stage and a larger number of engines are shown in the design stage, the mortality rate among the design and development engines is high and only a few of these reach production. Afterburning static sea-level thrust is plotted against completion of the 150 hour test in figure 1(b). In the 1959-1960 period engines are planned with afterburning sea-level static thrust ranging from 3,500 to 45,000 pounds.

Specific thrust. - The variation of sea-level static thrust per pound of air at "military" rated conditions with turbine inlet temperature for engines of various compressor pressure ratios is shown in figure 2. Curves of the variation of thrust per pound of air with turbine inlet temperature are shown for three compressor pressure ratios, assuming a high level of component efficiency. Although engine pressure ratios are not identified for each engine, the curves serve to bracket the engines shown. Several engines have turbine inlet temperatures of 2,000° F and show the theoretically expected increase in thrust per pound of air with increased turbine inlet temperature. Figure 3 presents the ratio of the specific thrust of each engine to its theoretical thrust. The data show the distribution of component efficiencies relative to a theoretical level for the various engines.

The variation in maximum thrust per pound of airflow at sea-level static conditions (afterburner operating) with turbine inlet temperature is presented in figure 4. In order to illustrate the effect of turbine inlet temperature on thrust per pound of airflow for a given set of conditions, theoretical performance for an afterburner temperature of 3040° F and a compressor pressure ratio of 8 has been plotted in this figure. In general, the data show increasing thrust per pound of air with increasing turbine inlet temperature. At any given temperature the maximum spread in the data of about ±10 percent is attributed to both the range in compressor pressure ratio and the range in afterburning temperatures for the engines shown.

Augmentation ratio is often used as a basis for comparing engine performance. The plot of thrust per pound of airflow against augmentation ratio in figure 5 shows that thrust augmentation ratio in itself is not useful in comparing different engines. For example, engines A and B shown in figure 5 have the same thrust augmentation; however, the specific thrust for engine B is 20 percent higher than for engine A. Engine C, which has a thrust augmentation of approximately 35 percent as compared to engine D with a value of over 60 percent, has a specific thrust of approximately 13 percent greater than engine D.

Airflow. - Figure 6 presents the sea-level static airflow for each engine plotted against completion date of the 150 hour qualification test. The thrust increases indicated in figure 1 are principally the result of increases in airflow with time as shown in figure 6. The solid line indicates the maximum airflow of the engines available at any given time. The broken line is taken from reference 1. The difference between the broken and solid line results from the additional time needed to complete the 150 hour qualification test over that previously estimated in reference 1.

Increases in static sea-level engine airflow shown in figure 6 are due to increases in airflow per unit of compressor frontal area or increases in compressor frontal area. The theoretical relation between air-handling capacity of the compressor, effective compressor inlet Mach number and compressor hub-tip radius ratio is shown in figure 7. The compressor frontal area is based on the area swept by the compressor blade tips. The compressor hub-tip ratios for most of the engines considered range from 0.4 to 0.55 and the effective inlet Mach numbers from 0.4 to 0.65, resulting in the flow capacity per unit of compressor tip frontal area varying from 22 to 36 pounds per second per square foot. The higher airflow handling capacities are for the design engines. Most of the design engines shown in figure 7 have a transonic compressor.

The development of the transonic compressor made possible values of mass flow well beyond 30 pounds per second per square foot of compressor frontal area. In making a transition from the conventional subsonic axial-flow compressor to a transonic compressor, airflow increases on the order of 40 percent are theoretically available. Further increases in effective compressor inlet Mach number (beyond 0.7) or decreases in hub-tip radius ratio (below 0.3) will yield small gains in airflow per unit of compressor tip frontal area. Compressor design technology, with respect to airflow handling capacity, is approaching a point of diminishing returns.

Airflow per square foot of compressor tip area is plotted against estimated date of completion of 150 hour test in figure 8. The broken curve shown in figure 8 represents data available in 1951 (ref. 1). Figure 8 illustrates the time periods during which the airflow advances discussed in figure 7 will occur for engines in the development and design stage. Design engines are grouped in the airflow bracket between 30 and 36 pounds per second per square foot. Engines in the development stage cover a range of airflow from 25 to 33 pounds per second per square foot of compressor tip frontal area. Engines currently in production range from 22 to 26 pounds per second per square foot of compressor tip area.

The air-handling capacity of the compressor based on the engine envelope area, including accessories, is presented in figure 9. The

curve represents the upper boundary of the data plotted. Here again, a definite increase in the maximum air-handling capacity, which would be expected from figure 8, is shown with increasing time. Engines in the design stage have values that vary from the order of 10 to as high as 23 pounds per second per square foot of engine envelope area. Values for engines in the development stage vary from 8 to as high as 18 pounds per second per square foot of engine envelope area. Engines in the production stage vary from 8 to as high as 15 pounds per second per square foot of engine envelope area.

Engine envelope area divided by compressor tip area is plotted against estimated completion data of the 150 hour test in figure 10. The spread in figure 10 is greatest for design engines. The large spread in the data indicates the need for caution when making airplane performance analyses which are dependent upon assumed values for the ratio of engine envelope area to compressor tip area.

The ratio of thrust (sea-level static nonafterburning) to engine envelope area (which is significant from a nacelle-drag standpoint) is plotted against estimated time of completion of the engine 150 hour qualification test in figure 11(a). Production engines vary from 500 to 1000 pounds of thrust per square foot of engine-envelope frontal area. Development engines vary from 700 to 1200 pounds per square foot of engine-envelope frontal area. Design engines vary from 700 to 1400 pounds per square foot of engine-envelope frontal area. A plot of the ratio of sea-level static afterburning thrust to engine envelope area with estimated completion of the 150 hour test is presented in figure 11(b).

Specific fuel consumption at sea-level static conditions based on military-rated thrust with estimated completion of the 150 hour test is plotted in figure 12. The broken curve is representative of the data presented in reference 1. A wide range of specific fuel consumption for the engines is indicated. The large spread in specific fuel consumption values for design engines is largely the result of the range of turbine inlet temperatures that are being considered for these engines. Higher turbine inlet temperature results in higher specific fuel consumption.

In order to remove the effects of turbine inlet temperature and compressor pressure ratio and permit the specific fuel consumption values to reflect only changes in component efficiencies, theoretical performance was computed for each engine. The ratio of theoretical performance to actual performance is plotted in figure 13. Values of this ratio greater than unity represent actual component efficiencies higher than those selected for the theoretical calculations.

The variation in specific fuel consumption with compressor pressure ratio at sea-level static conditions is shown in figure 14. The broken

curve is taken from reference 1. Two theoretical turbine-inlet-temperature lines are shown, one at 1500° F and the other at 2000° F.

Specific engine weight. - The figures discussed so far have presented data on sea-level static thrust and airflow for production, development and design engines. The next series of figures are directly concerned with engine specific weight and relate the importance of airflow increases and engine weight reductions to sea-level static specific engine weight.

In figure 15 specific engine weight is plotted against estimated completion time of the 150 hour test. The figure indicates a reduction in specific engine weight with time from that originally presented in reference 1. The change in specific engine weight with time for engines without afterburners is shown in figure 15(a). Values for production engines are around 0.43, those for development engines range from 0.3 to 0.4 and those for design engines range from 0.1 to 0.25.

In figure 15(b) the variation of engine specific weight with time for engines with afterburners is shown. The sea-level static thrust is based on the afterburner not operating (military-rated thrust). Values for production engines are around 0.5, those for development engines range from 0.35 to 0.5 and those for design engines range from 0.2 to 0.4.

Figure 15(c) presents the variation of specific engine weight with time for the condition where the engine weight includes the afterburner weight and the thrust is based on the afterburner operating. Values for production engines are around 0.3, those for development engines range from 0.23 to 0.38, and those for design engines range from 0.1 to 0.23.

Specific engine weight is plotted against thrust in figure 16. Data for nonafterburner engines are shown in figure 16(a). Specific weight values for design engines are essentially 0.23, except for engines in the 2500 pound thrust class, which are about half of this value. Variation of specific weight for the afterburner engines with the afterburner not operating (military-rated thrust) is shown in figure 16(b). The level of specific weight increased to a value around 0.30 for the design engines due to the addition of the afterburner weight. Variation of specific weight with sea-level static afterburning thrust (maximum thrust rating) is presented in figure 16(c). Because the thrust increase approximately balanced the additional weight, the addition of the afterburner when operating resulted in little or no decrease in sea-level static specific engine weight over that obtained with nonafterburning engines.

Weight to airflow ratio. - The variation in the ratio of engine weight to air-handling capacity with sea-level static thrust for

nonafterburning engines is presented in figure 17. The data in figure 17 show about 40 percent reduction in this ratio in going from production to design engines.

Engine Weight

Turbojet engine weight. - Engine weight is plotted against compressor tip diameter cubed in figure 18. Compressor tip diameter to the cube power was used as the correlating parameter to illustrate the approximation of geometric similarity between the different engine sizes.

Current data are arranged into two classes: (1) data for engines without afterburners, and (2) data for engines with afterburners.

For engines without afterburners the cubic curve which best fits the data can be expressed by the equation:

$$W_e = 0.089\ D_{ct}^3$$

where

W_e engine dry weight, lb

D_{ct} compressor tip diameter, in.

For engines with afterburners, the curve which best fits the data can be expressed by the equation:

$$W_e = 500 + 0.089\ D_{ct}^3$$

Although this latter equation implies that an afterburner weighs 500 pounds more than the nonafterburner tailpipe regardless of size, the scatter in the data precludes making a definite conclusion as to the effect of size on afterburner weight.

Turbojet component weights. - Figures 16 and 17 show that the specific weight and the ratio of weight to airflow for design engines are markedly reduced from values for production and development engines. In order to determine if this reduction could be attributed to any particular component, the weight distribution by component was plotted in figure 19. Because of the lack of component weight data on all engines, this figure is not as complete as figure 18. The engine-component weight distribution for nonafterburner engines is shown in figure 19(a). The components listed are the inlet, compressor, combustor, turbine, tailpipe, and accessories and controls.

Although there is a fairly wide spread in the data, no trend in weight distribution is seen going from production and development engines to design engines. The engine-component weight distribution for afterburning engines is presented in figure 19(b). It is interesting to note that this figure indicates that afterburners weigh about 15 percent of the total engine weight more than the tailpipe they replace. Although not in exact agreement with the conclusion drawn from figure 18, the area of disagreement is within the spread in the data and is probably caused by the difference in sample size.

Because of the lack of trend in weight distribution, the possibility of obtaining engine-component weight relations was next studied. Figures 20 to 22 present the weight data for each component and show a relation for each component weight in terms of a correlating dimensional parameter.

Figure 20 presents the variation of the weight of the compressor plus turbine as a function of the compressor tip diameter cubed. The cubic relation which best fits the data is as follows:

$$W_{c+t} = 0.0602\ D_{ct}^{3}$$

where

W_{c+t} weight of compressor plus turbine, lb

D_{ct} compressor tip diameter, in.

The data group closely for the small engines, although the percentage deviation of the data at the lower end of the curve is high.

The variation of turbine weight with turbine tip diameter cubed is presented in figure 21. The weight relation which best fits the data is:

$$W_{t} = 0.02\ D_{tt}^{3}$$

where

W_{t} weight of the turbine, lb

D_{tt} turbine tip diameter, in.

An attempt to correlate the turbine weight per stage resulted in more scatter than the above relation. The lack of correlation with number of stages may be due to the small sample size and lack of any method to evaluate design ingenuity.

[redacted]

The variation of compressor weight with compressor tip diameter cubed is presented in figure 22. The data approximate a weight relation for the compressor as follows:

$$W_c = 0.037\ D_{ct}^3$$

where

W_c compressor weight, lb

D_{ct} compressor tip diameter, in.

The attempt to correlate compressor weight with length was not satisfactory, which again may be due to the limited amount of data. No attempt was made to correlate compressor weight with number of stages. In each of the above weight relations, design engines show somewhat lower weights from those shown for production and development engines.

Ram-jet engine weight. - The variation of ram-jet engine weight (including the inlet and exit nozzle) divided by ram-jet length (also including inlet and exit nozzle) with combustion-chamber diameter is presented in figure 23. Engine diameters range from 20 to 50 inches for the data presented in this figure. The weight relation is affected by altitude design at a given Mach number. For example, engines A and B (fig. 23) have the same thermodynamic design, but are considerably different in weight. Engine A, designed for lower altitude, required a heavier structure. The lack of a sufficient number of engines designed for the same flight condition makes correlation on a dimensional basis fairly meaningless. The only conclusion that can be drawn from figure 23 is that for ram-jet engines from 20 to 50 inches in diameter, the ratio of weight to length is from 3 to 6 pounds per inch.

Flight Performance

Previous compilations of comparative engine performance data such as reference 1 have generally presented only sea-level static performance. In some engines currently in the design stage, design procedures intended to improve engine performance at flight conditions make comparisons of sea-level static performance misleading.

The air-handling capacity, over-all engine efficiency, and several other parameters that reflect the flight performance of turbojet and ram-jet engines are presented in figures 24 to 32 and are discussed in the following paragraphs. For all engines shown, flight performance was calculated using the ram-pressure recovery ratio shown in figure 24.

Flight performance data, combined with the sea-level static performance presented in a previous section of this report will provide information on engine test facility capacity requirements for turbojet and ram-jet engines.

Turbojet flight performance. - The variation in net thrust per pound of airflow with flight Mach number at 35,000-foot altitude is presented in figure 25 for several turbojet engines. The thrust in figure 25(a) is based on military-rated speed and temperature and the exit nozzle for all engines shown is convergent-divergent. The higher values of thrust per pound of airflow for the two upper curves are attributed to higher turbine inlet temperatures, 1850° and 2000° F. Figure 25(b) shows the variation in maximum net thrust per pound of air with flight Mach number for afterburning turbojet engines. A convergent-divergent nozzle is assumed.

The variation of thrust per pound of air with flight Mach number for some of the engines with convergent nozzles at military-rated conditions is shown in figure 25(c). The thrust per pound of air at a given flight Mach number for a given engine with a convergent exit nozzle is lower than that shown in figure 25(a) for the same engine with a convergent-divergent nozzle. This same trend is shown in figure 25(d) where the variation in maximum thrust (afterburner operating) can be compared with that in figure 25(b). The data illustrate the performance gains available in applying a convergent-divergent exit nozzle to the engine over that obtained with a convergent nozzle, particularly at the higher Mach numbers.

The variation in corrected airflow with flight Mach number is presented in figure 26. Most of the engines are grouped closely in spite of the fact that the engines shown are design, development, and production engines. Performance data for most of the engines end at around Mach 2. Airflow data for four engines are shown up to a Mach number of 3.2. With the exception of two engines, the engines operate at constant mechanical speed. Two engines operate at constant aerodynamic speed over part of the Mach number range and therefore the corrected airflow is maintained at or near a value of unity up to a Mach number of about 2.0 and then decreases at higher Mach numbers. This increase in air-handling capacity will increase the thrust output and thus does significantly reduce specific weight under flight conditions.

The variation in over-all engine efficiency with flight Mach number is presented in figure 27. The afterburner performance is shown in figure 27(a) and the nonafterburner performance is presented in figure 27(b). The engines shown in figure 27(a) have not quite achieved the high theoretical performance level indicated for a turbine inlet temperature of 2000° F, although several engines are quite close. The data show the important engine efficiency increases occurring with increasing flight Mach number. At a Mach number of 3.2, the engine efficiency

of two afterburning engines in the design stage has reached a value of over 34 percent. The nonafterburner performance shown in figure 27(b) is considerably higher than that shown in figure 27(a) for any flight Mach number. At a flight Mach number of 2.0, for example, the over-all engine efficiency for afterburning engines is about 22 percent, while for nonafterburning engines, the value is about 33 percent, or an increase of about 50 percent in engine efficiency in going to the nonafterburner engine.

The varition in thrust ratio (ratio of net thrust at 35,000 feet to sea-level static net thrust) with flight Mach number is shown in figure 28. Performance for afterburner engines is shown by solid lines and that for nonafterburner engines is shown by broken lines. The data group quite closely for engines in the development and design stage.

The variation in specific engine weight with flight Mach number is shown in figure 29. Afterburner engine performance is presented in figure 29(a) and nonafterburner engine performance is presented in figure 29(b). From the data it is not possible to determine which factor in this variable (engine weight, thrust per pound of airflow, or airflow differences under flight conditions) is the major cause of the large spread.

Ram-jet flight performance. - The variation in over-all ram-jet engine efficiency with flight Mach number is presented in figure 30. Several theoretical curves are presented for different combustion temperature levels. With few exceptions, the over-all efficiency of the ram-jet engine is considerably below the theoretical level. The ram-jet engine, unlike the turbojet, has yet to achieve the potential over-all efficiency available as shown by the theoretical performance. Concentrated research and development in altitude research facilities can increase the performance level. Engine A (fig. 30) was subject to intensified development in an altitude facility and has achieved a high level of performance.

The variation in ram-jet engine thrust per pound of airflow with flight Mach number is presented in figure 31. The data plotted for the ram-jet engines fall within the theoretical performance shown for combustion temperatures in the range from 2040° to 3040° F.

The variation in ram-jet engine specific weight with flight Mach number is presented in figure 32. The ram-jet engine weight includes the inlet system and exit nozzle together with all controls and accessories. The specific-weight advantage of the ram-jet engine over the turbojet engine can be appreciated from this figure. For example, at a flight altitude of 35,000 feet and Mach number of 3.0, a representative turbojet specific engine weight would be about 0.135 (fig. 29(a)), whereas for a ram-jet at the same altitude and flight speed, the value would be about 0.065, or about a 55-percent reduction in specific weight from the turbojet value.

CONCLUSIONS

This report has presented a compilation and analysis of sea-level static and flight performance data for existing and designed U. S. axial-flow turbojet and ram-jet engines. The following general conclusions can be drawn:

1. An approximate linear increase of maximum nonafterburning sea-level static thrust with time of availability is indicated with thrust being increased from 10,000 pounds in 1950 to over 35,000 pounds in 1960. At any given time, a wide range of engine thrust exists. More design turbojet engines are now being supported than ever before.

4339

2. A major cause of increased thrust has been the increase in airflow capacity. The airflow capacity of the axial-flow compressor, while steadily improving, is approaching the area of diminishing returns because of the fundamental limit on flow through a given area. The flow capacity has increased from 22 pounds per second per square foot of compressor tip area to a value of 36 in the time period from 1954 to 1959. The majority of the design-engine compressors have a transonic first stage.

3. A major reduction in specific engine weight is indicated in going from production engines to design engines. The value for nonafterburner engines decreased from about 0.4 to about 0.23. Specific engine weights of about 0.1 are indicated for design engines in the 2500 pound thrust class. The reduction in weight seems to have been accomplished throughout the engine inasmuch as there was no significant trend in the component weight distribution going from production to design turbojet engines.

4. Flight-performance data for turbojets reflect a high level of thermodynamic gas generator performance. Major gains in performance in future turbojets are not to be expected through improvements in component efficiency. Constant-aerodynamic-speed compressor operation over part of the flight speed range and increased turbine inlet temperature show improved flight performance for some design engines.

5. Ram-jet flight-performance data reflect a low level of thermodynamic performance. Major performance gains in future ram-jets appear available through concentrated full-scale reseach and development.

[redacted]

APPENDIX - SYMBOL LIST FOR FIGURES

A_c compressor tip frontal area, sq ft

A_e engine envelope area, sq ft

C_v exhaust nozzle velocity coefficient

D_{ct} compressor first stage tip diameter

D_H/D_T compressor hub-tip ratio (ratio of compressor first stage hub diameter to tip diameter)

D_{tt} turbine last stage tip diameter

F net thrust, lb

P_3/p_2 compressor total pressure ratio

S.F.C. specific fuel consumption, W_f/F, (lb fuel/hr)/lb thrust

T_4 turbine inlet total gas temperature

T_9 afterburning total gas temperature, ^oF

W_a airflow rate, lb/sec

W_f fuel flow, lb/hr

ε correction factor (ref. 2) (ε = 1.0 assumed pressure losses balance corrections for hot gas)

η_b combustion efficiency

η_c compressor efficiency

η_e over-all engine efficiency

η_t turbine efficiency

Subscripts:

A.B. afterburner engine

4339

[redacted]

c	compressor
c + t	compressor plus turbine
e	engine
max	maximum rated conditions
mil	military rated conditions
N.A.B.	nonafterburning engine
sls	sea-level static

REFERENCES

1. Cesaro, Richard S., and Lazar, James: Graphic Analysis of American and British Axial-Flow Turbojet Engine Performance Trends (Current and Future). NACA RM 51K29, 1951.

2. Pinkel, Benjamin, and Karp, Irving M.: A Thermodynamic Study of the Turbojet Engine. NACA Report 891, 1947.

[redacted]

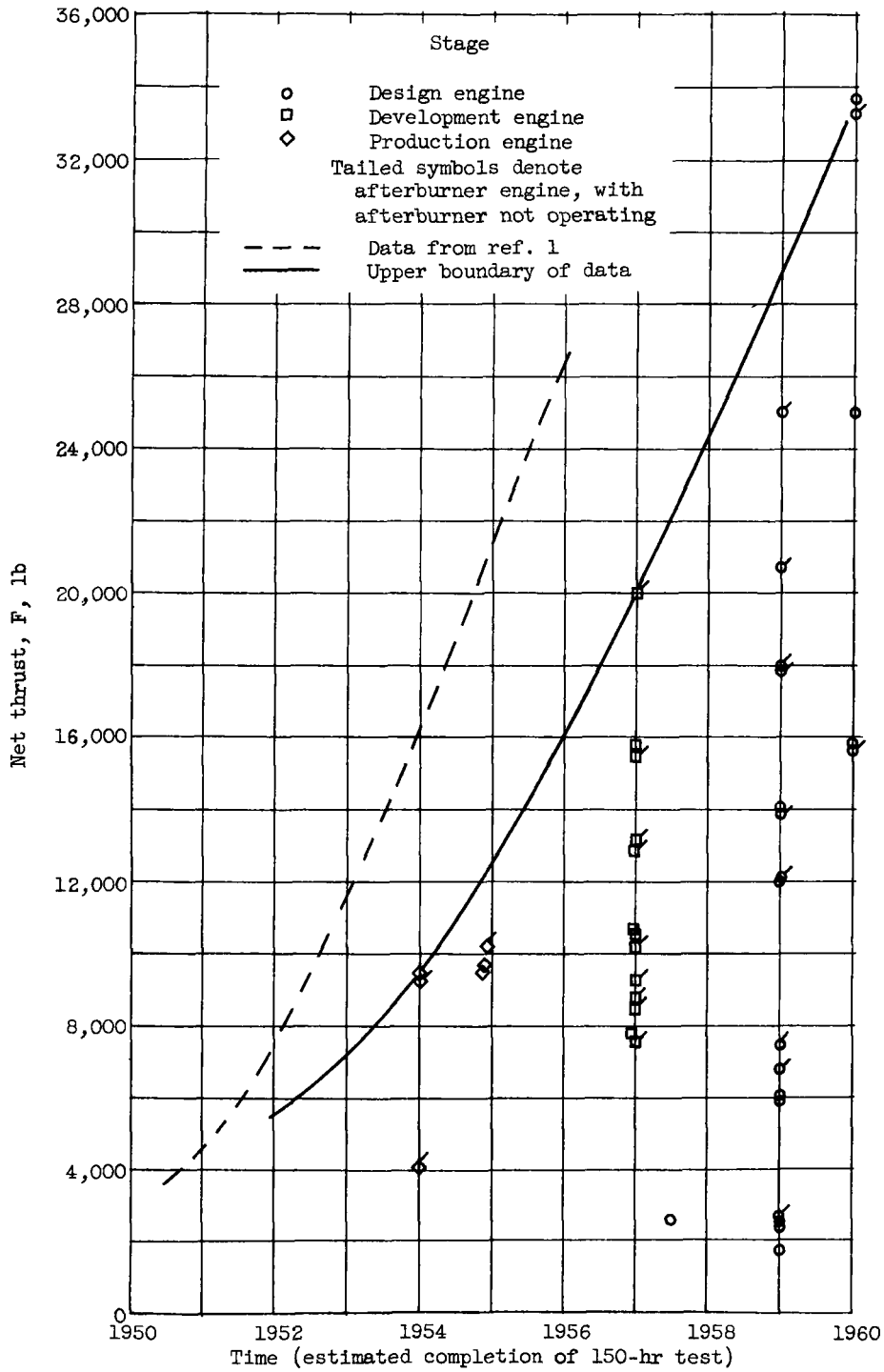

(a) Thrust without afterburner or with afterburner not operating.

Figure 1. - Engine sea-level static thrust at estimated completion time.

[redacted]

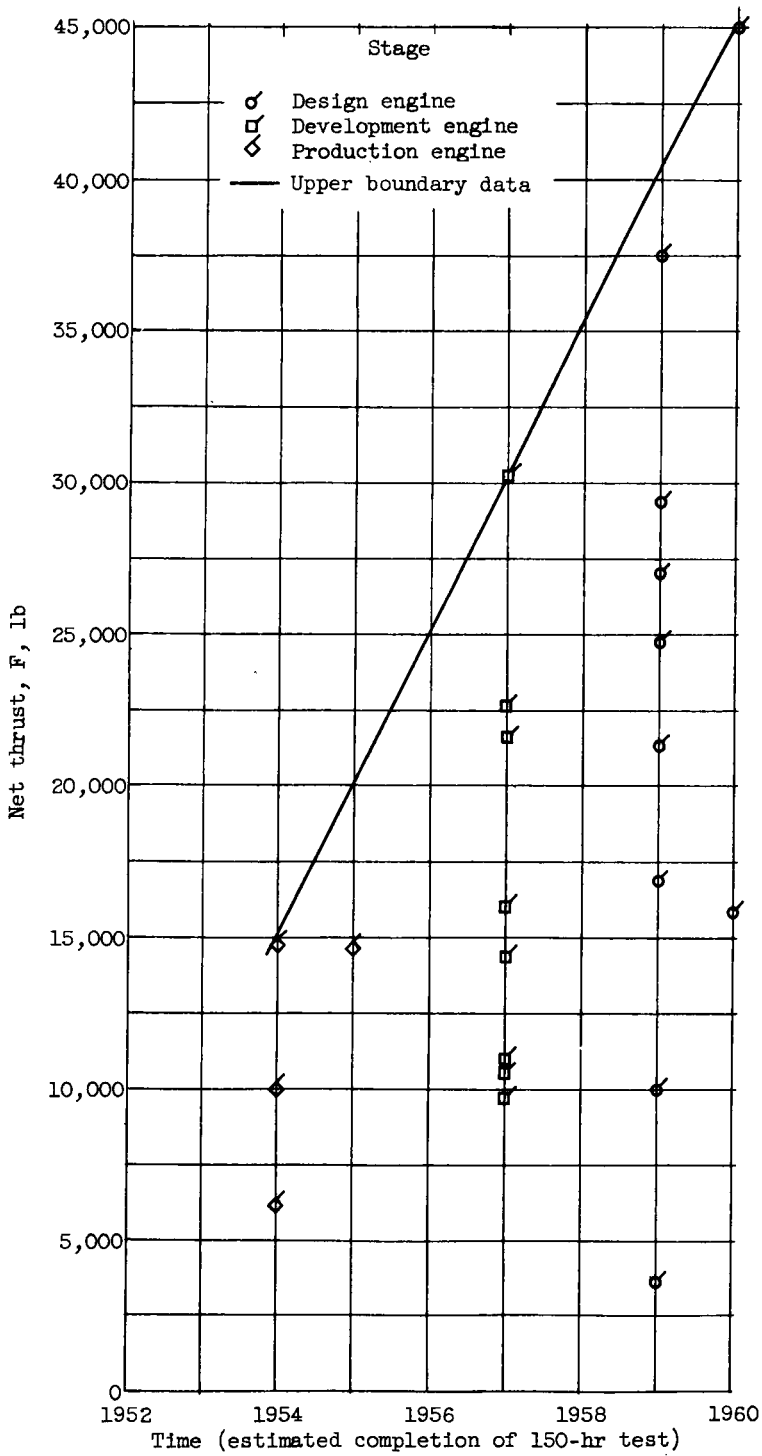

(b) Thrust with afterburner operating.

Figure 1. - Concluded. Engine sea-level static thrust at estimated completion time.

[redacted]

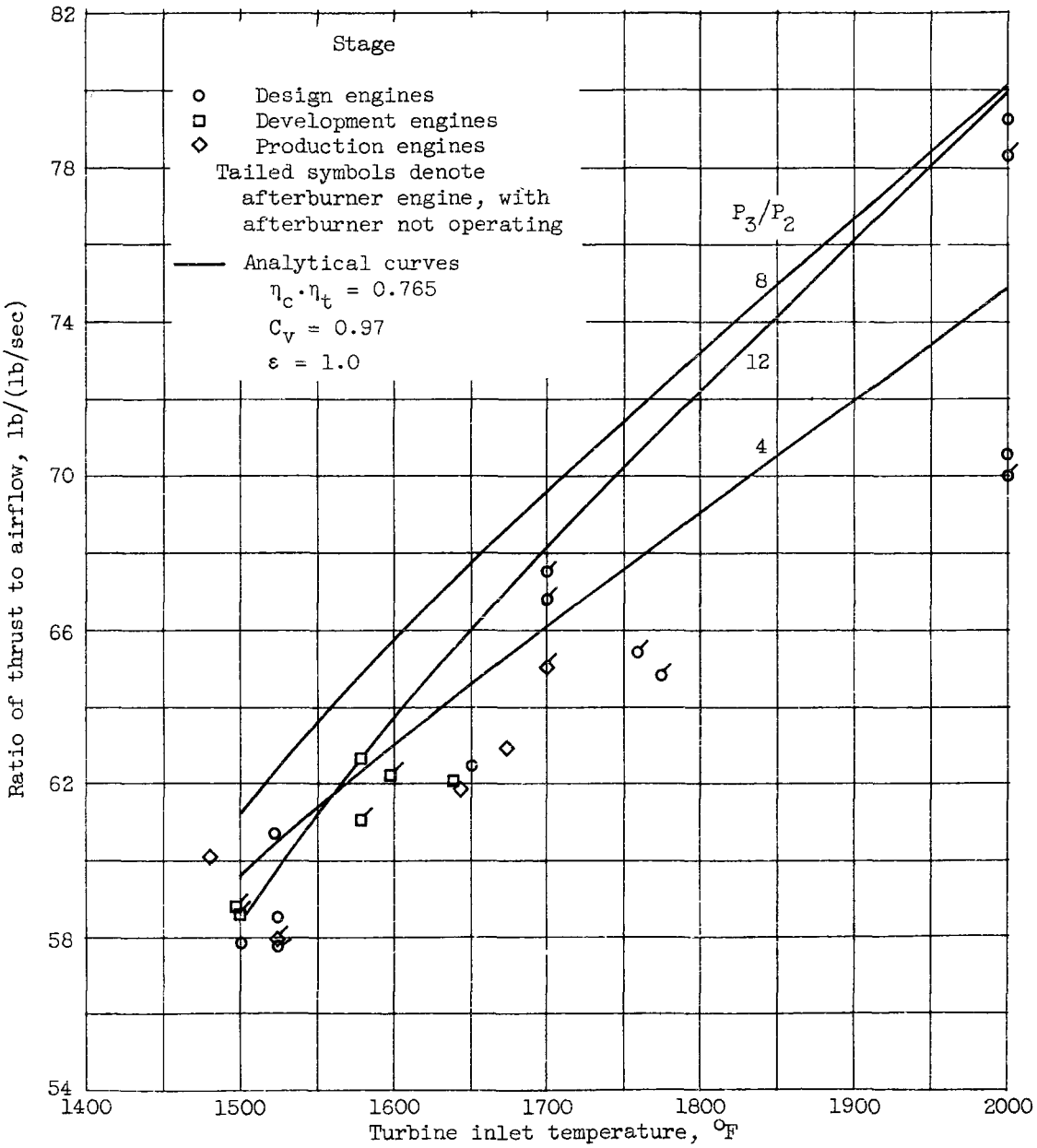

Figure 2. - Effect of turbine inlet temperature on specific thrust. Sea-level static conditions.

[redacted]

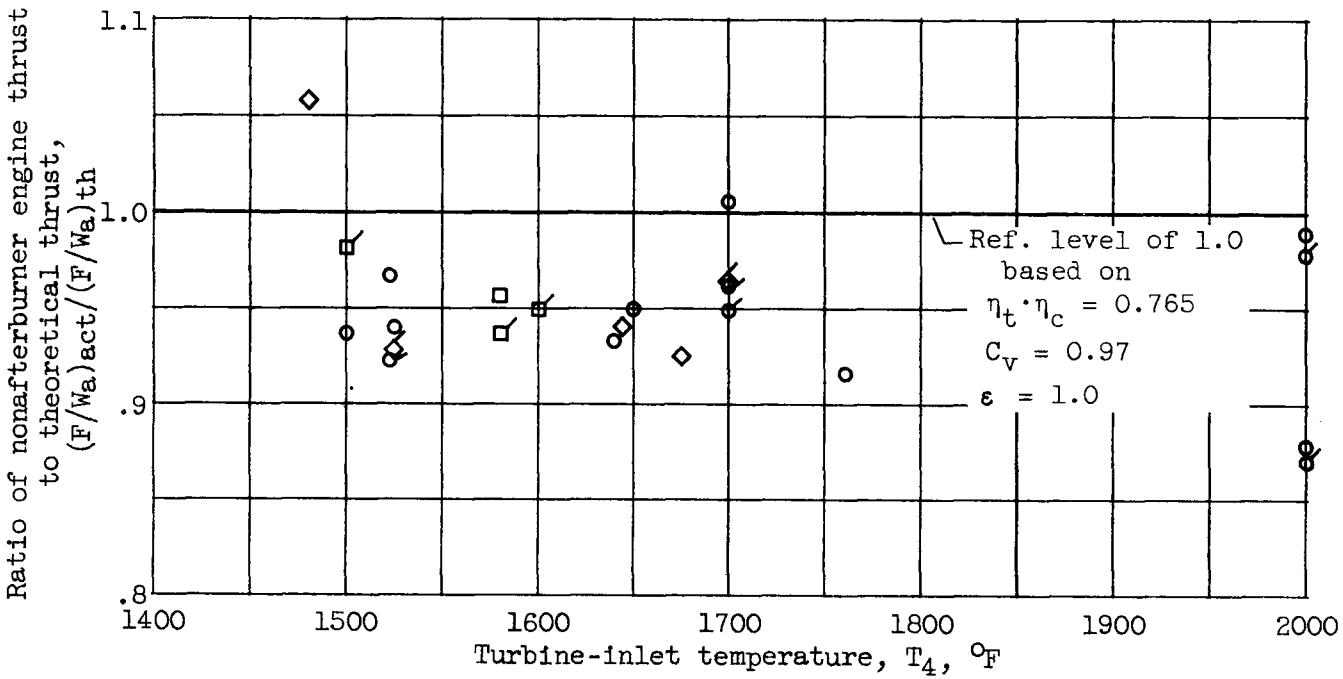

Figure 3. - Ratio of specific thrust to theoretical thrust plotted against turbine-inlet temperature. Sea-level static conditions.

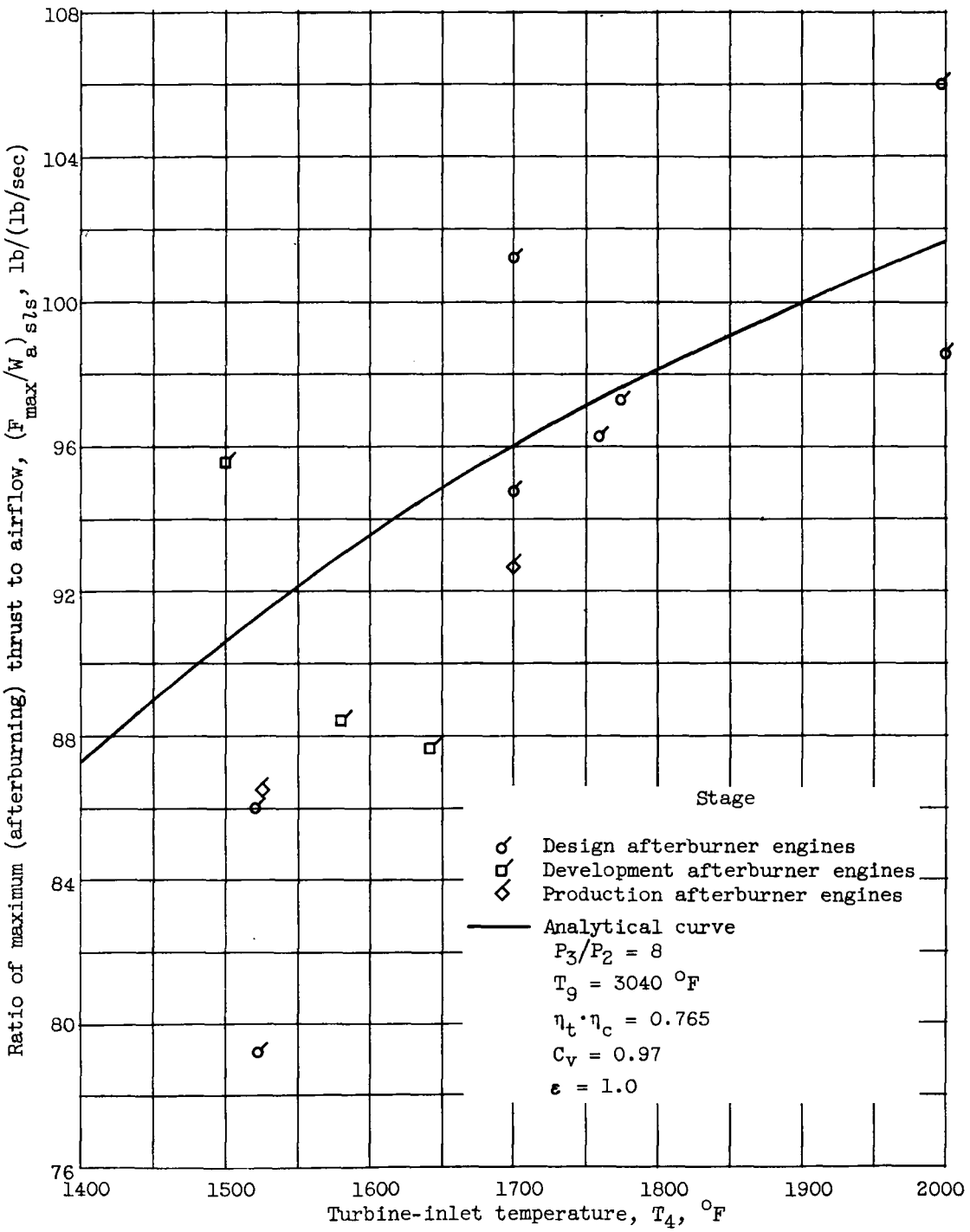

Figure 4. - Variation of maximum specific thrust with turbine-inlet temperature. Sea-level static conditions.

4339

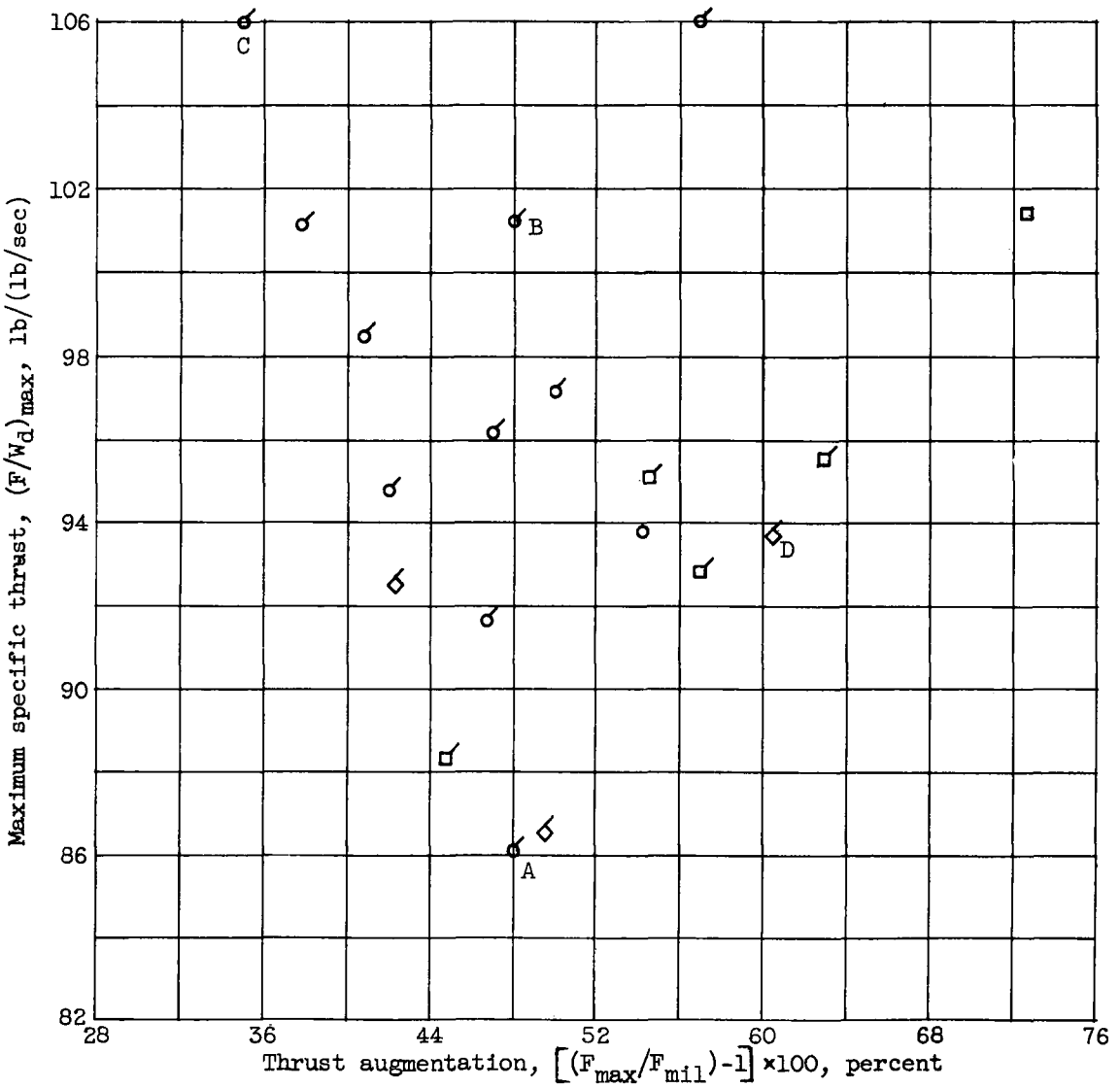

Figure 5. - Variation of maximum specific thrust with thrust augmentation. Sea-level static conditions.

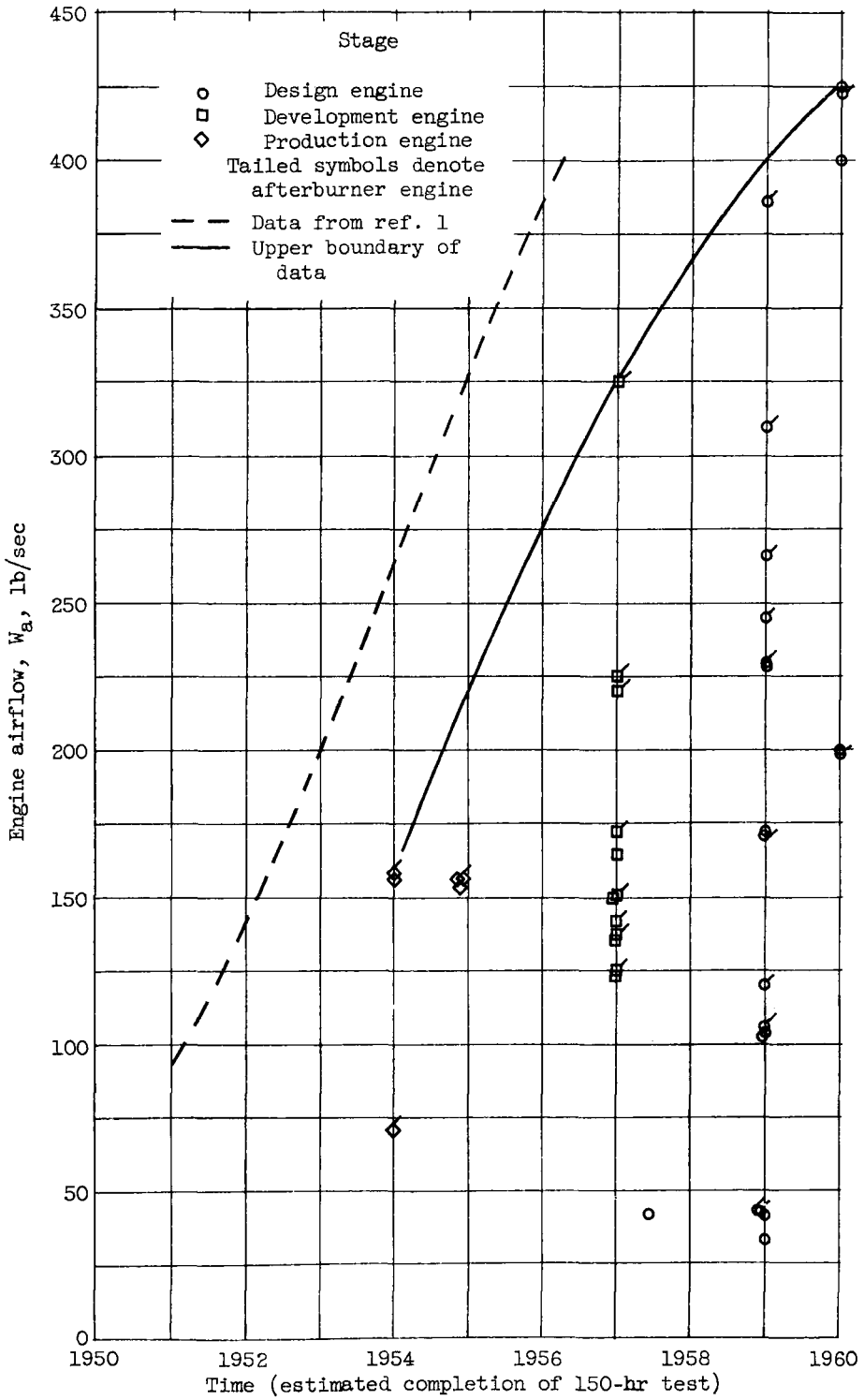

Figure 6. - Engine airflow at estimated completion time. Sea-level static conditions.

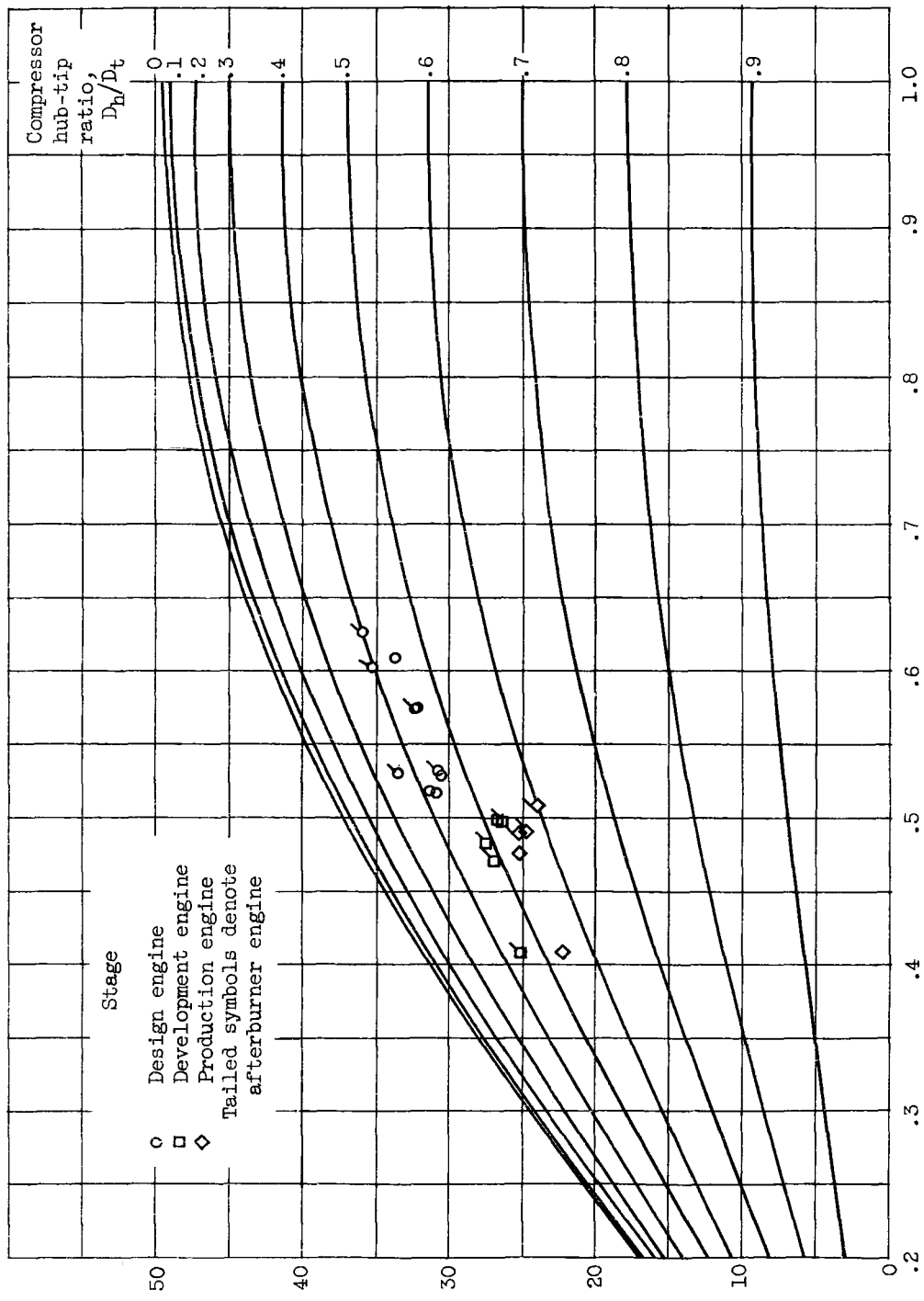

Figure 7. - Variation of ratio of airflow to compressor tip area with effective inlet Mach number. Sea-level static conditions.

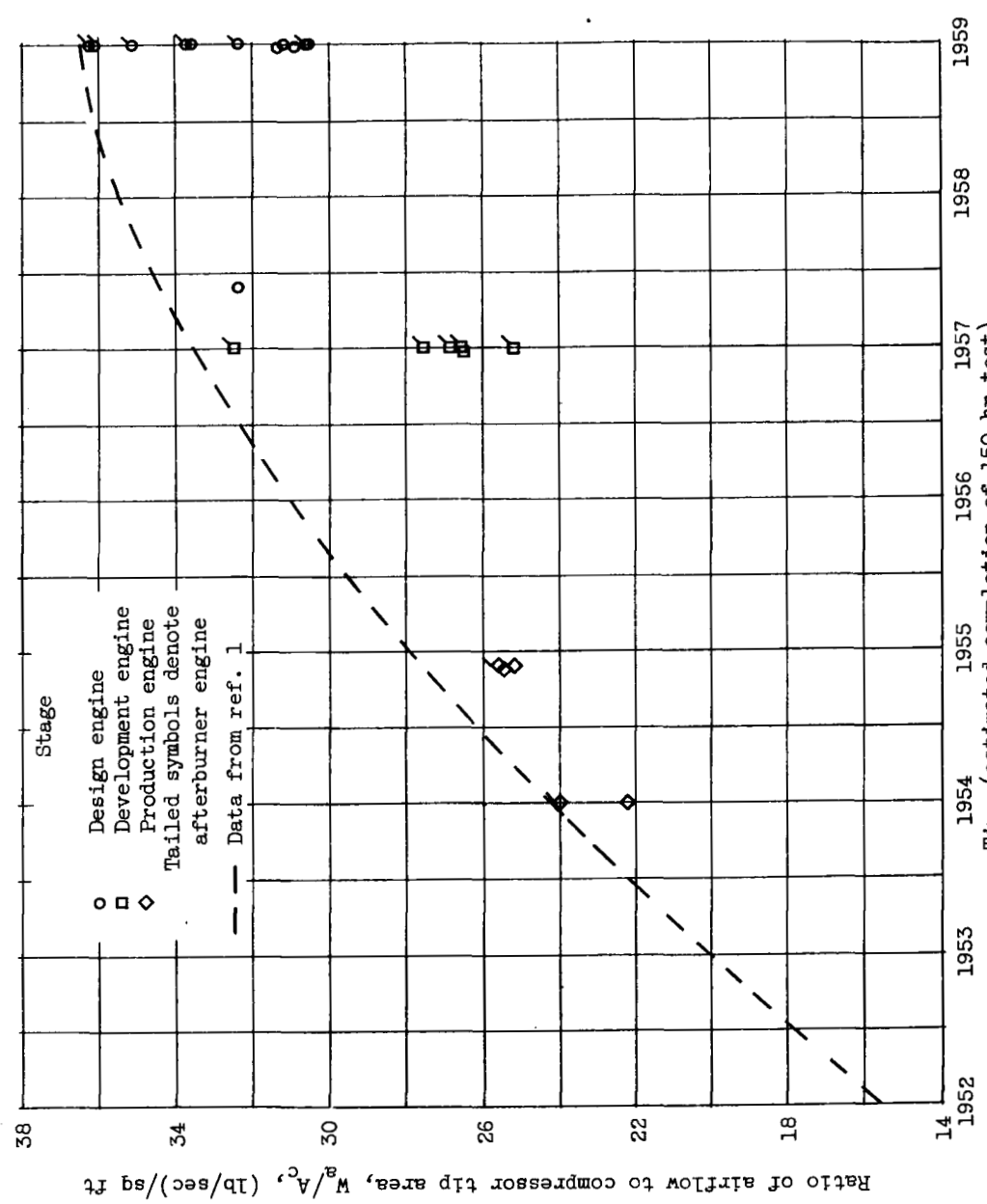

Figure 8. - Ratio of airflow to compressor tip area at estimated completion time. Sea-level static conditions.

4539

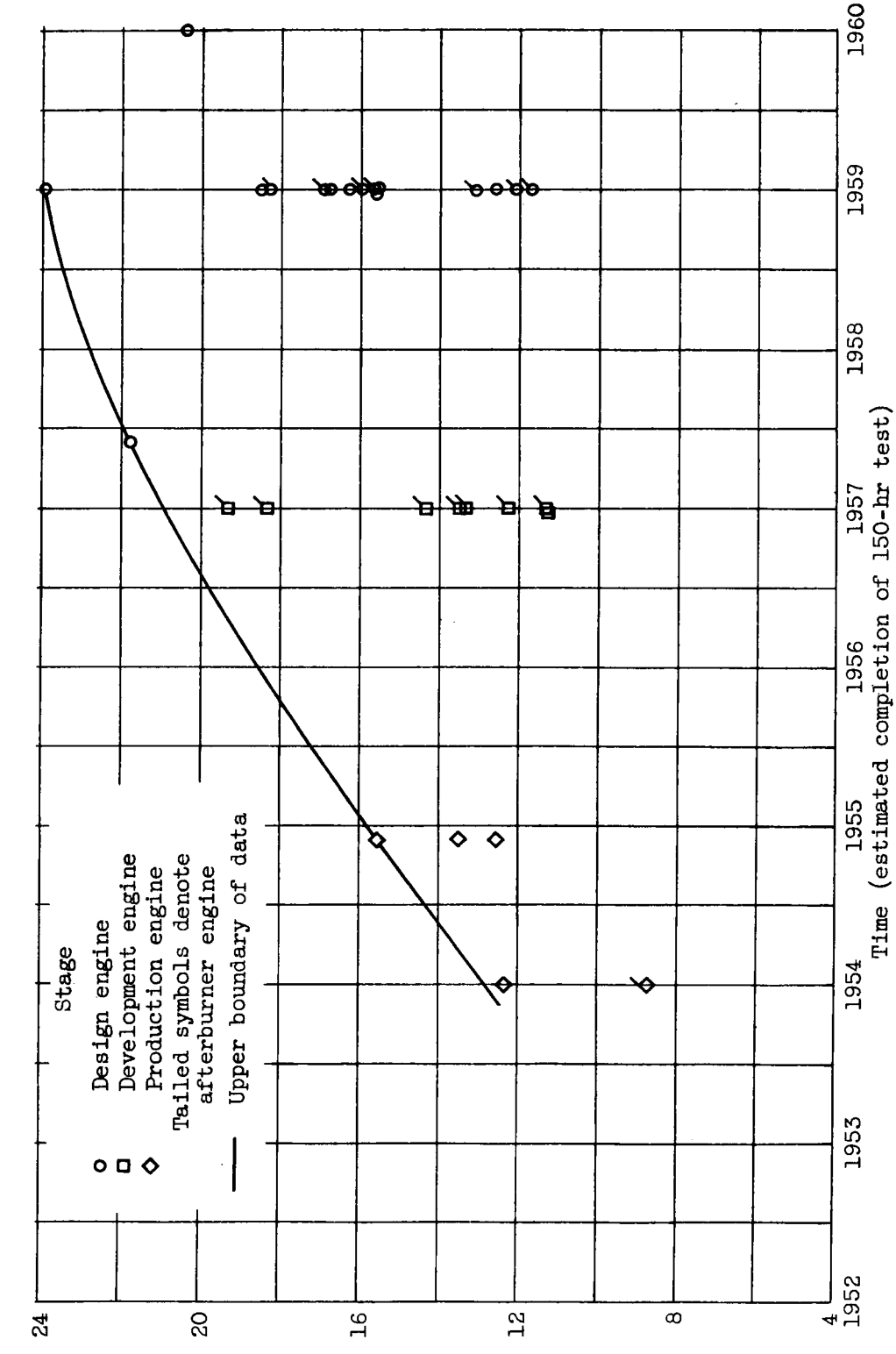

Figure 9. - Ratio of airflow to engine envelope area at estimated completion time. Sea-level static conditions.

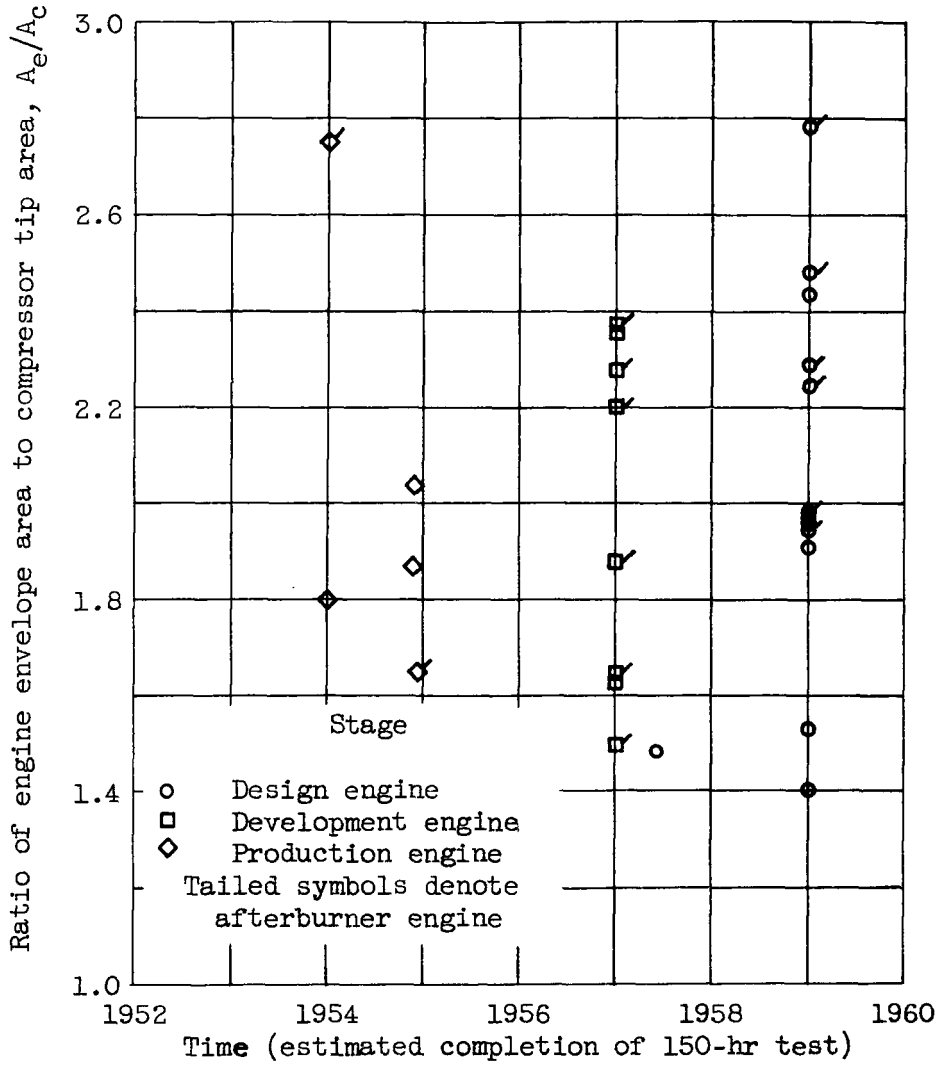

Figure 10. - Ratio of engine envelope area to compressor tip area at estimated completion time.

[redacted]

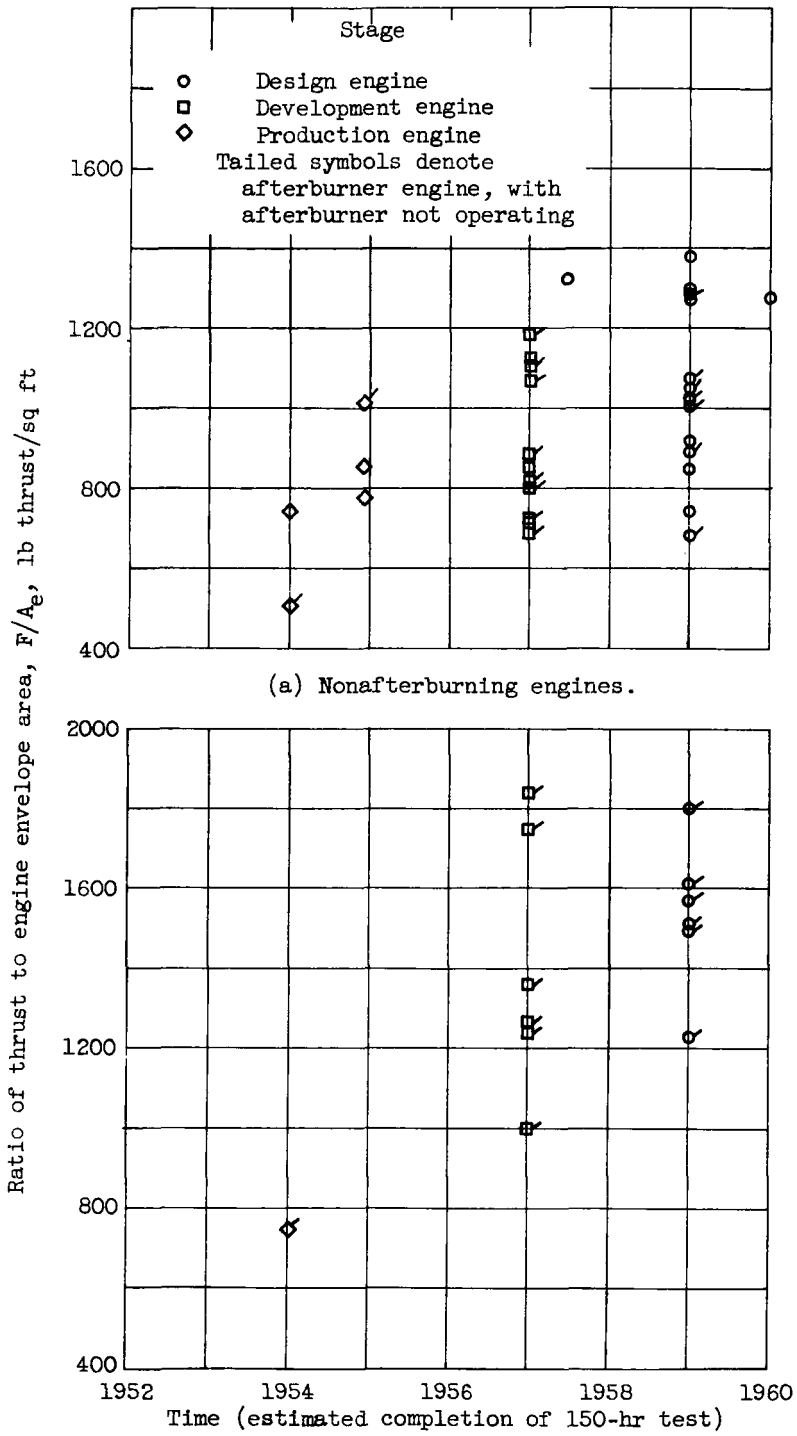

(a) Nonafterburning engines.

(b) Afterburning engines.

Figure 11. - Engine thrust per unit engine envelope area at estimated completion time. Sea-level static conditions.

[redacted]

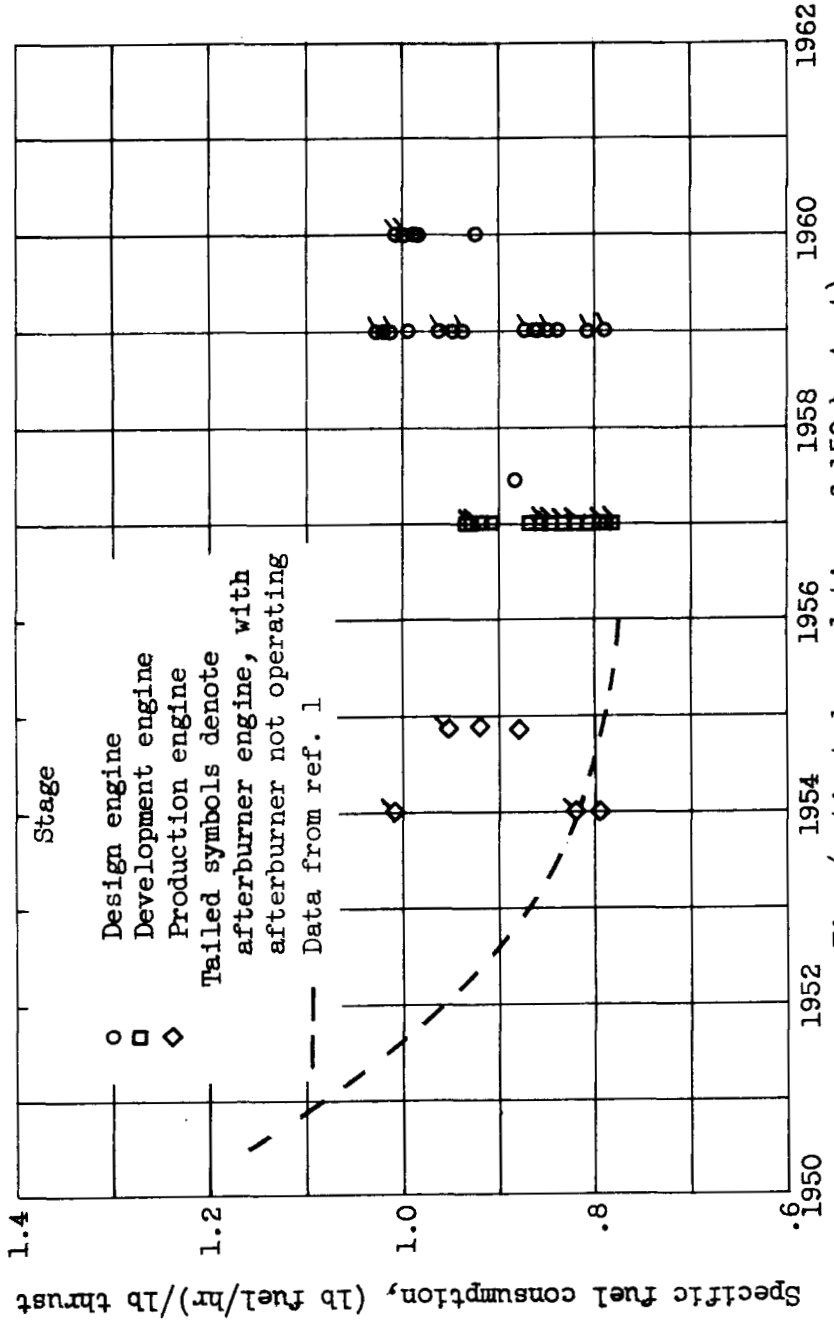

Figure 12. - Specific fuel consumption at estimated completion time. Sea-level static conditions.

4339

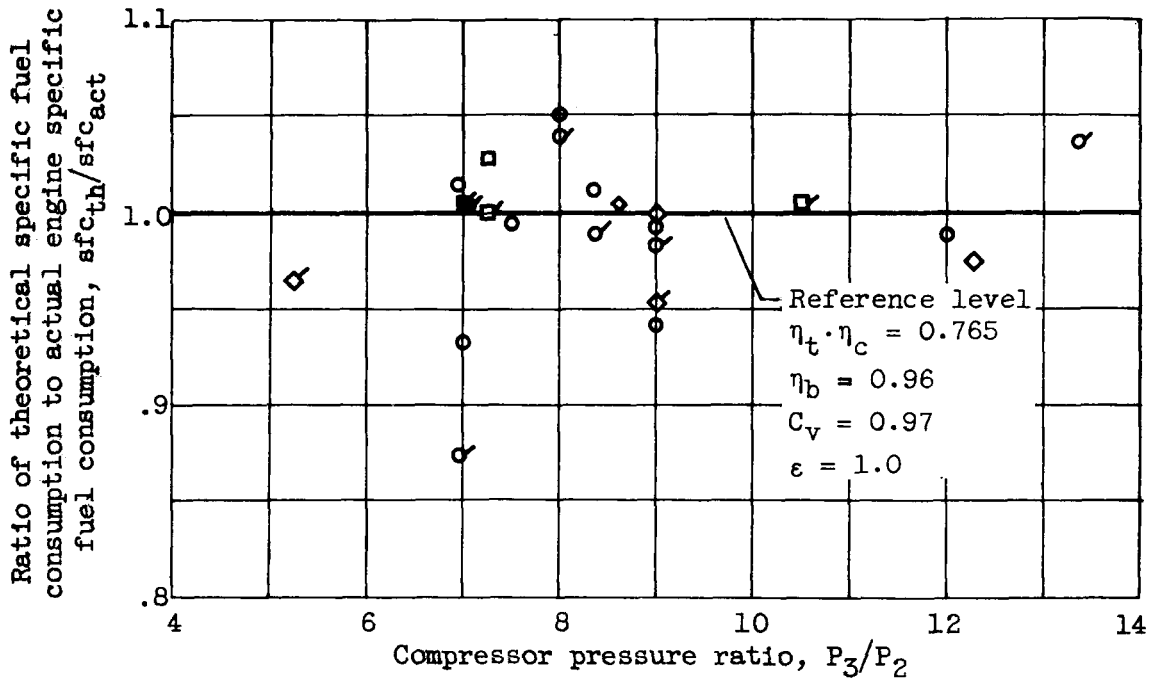

Figure 13. - Ratio of theoretical specific fuel consumption to actual specific fuel consumption plotted against compressor pressure ratio. Sea-level static conditions.

[redacted]

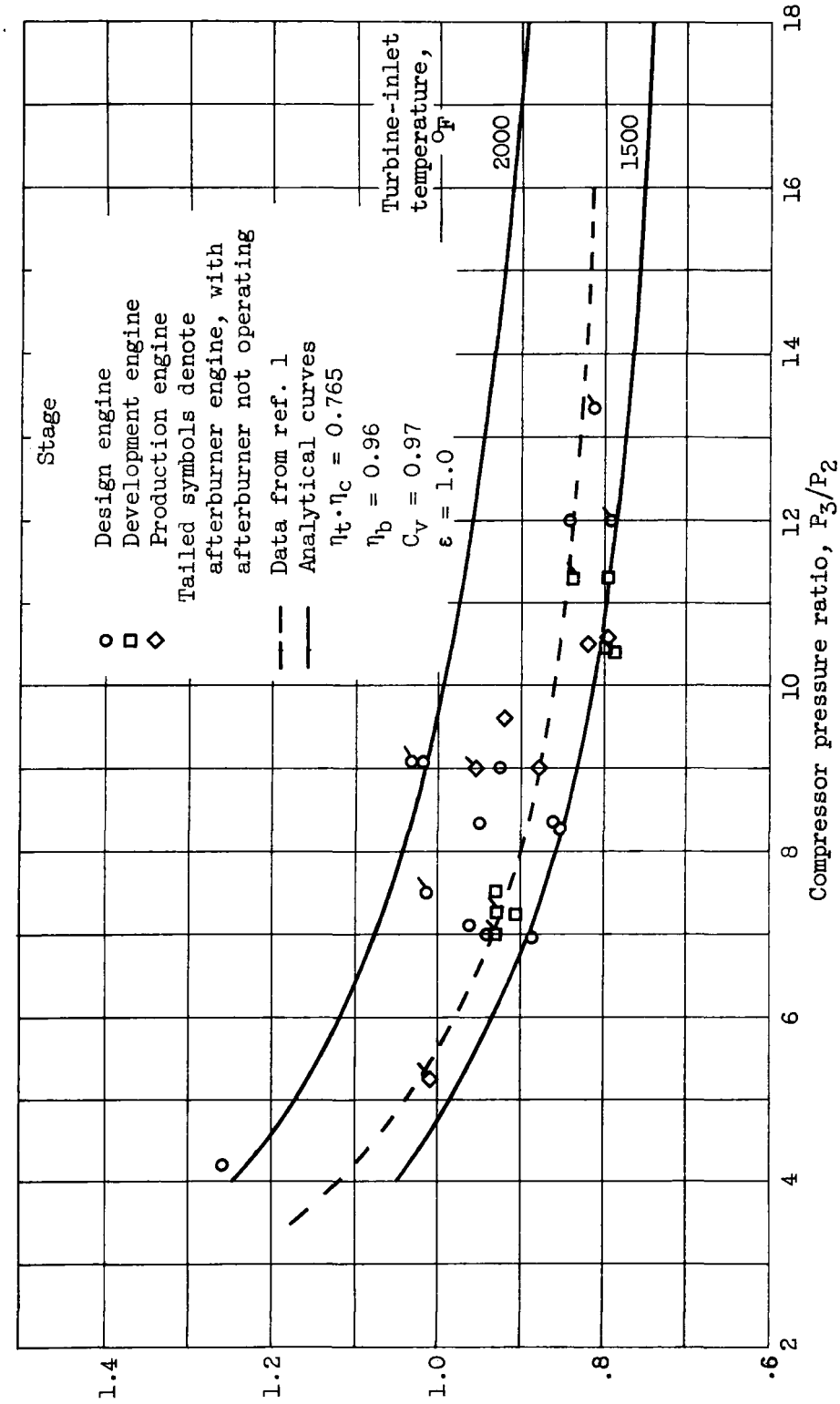

Figure 14. - Variation of specific fuel consumption with compressor pressure ratio at sea-level static conditions.

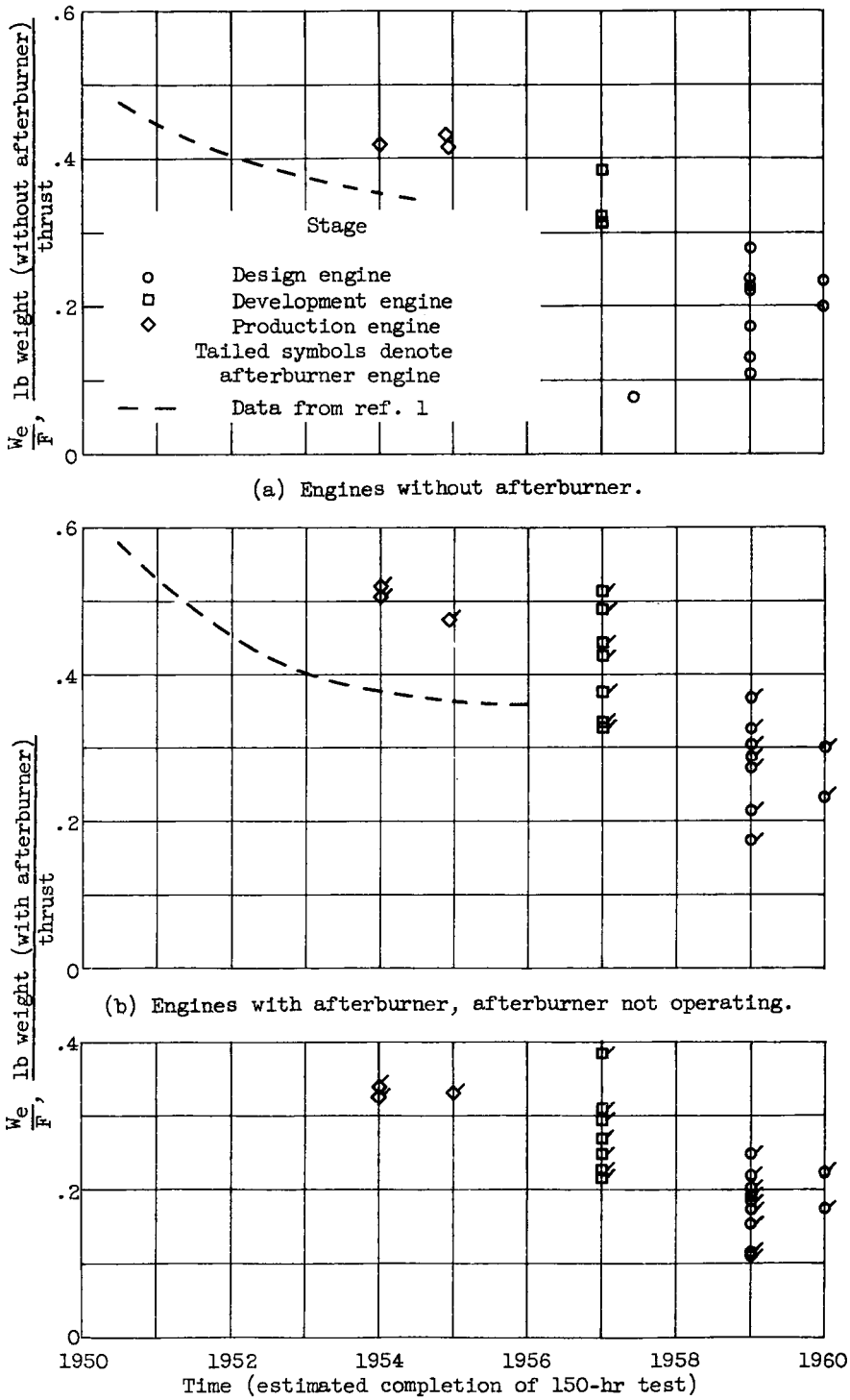

(a) Engines without afterburner.

(b) Engines with afterburner, afterburner not operating.

(c) Engines with afterburner, afterburner operating.

Figure 15. - Specific engine weight at estimated completion time. Sea-level static conditions.

[redacted]

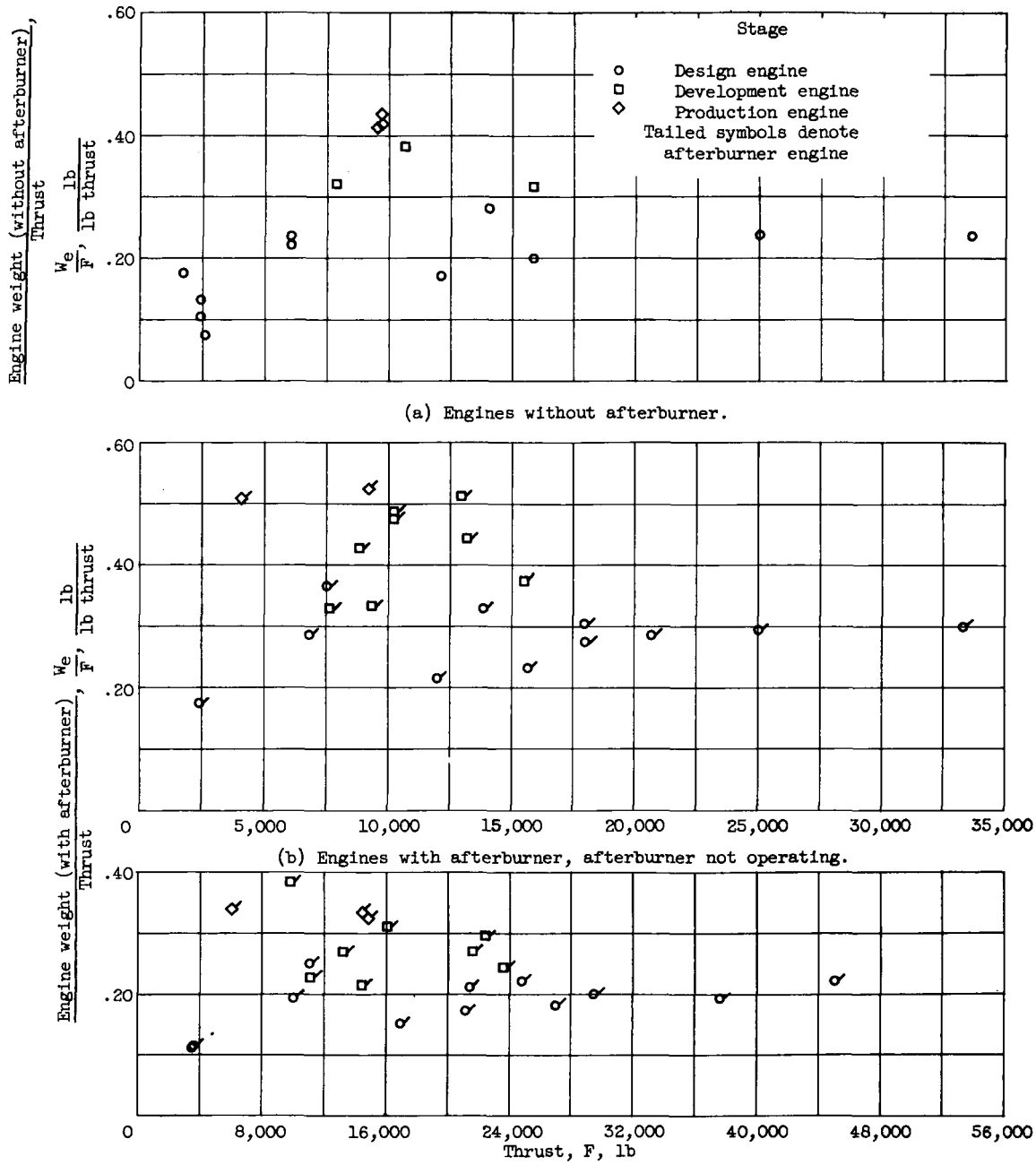

(a) Engines without afterburner.

(b) Engines with afterburner, afterburner not operating.

(c) Engines with afterburner operating.

Figure 16. - Variation of specific engine weight with thrust at sea-level static conditions.

CI-5

4339

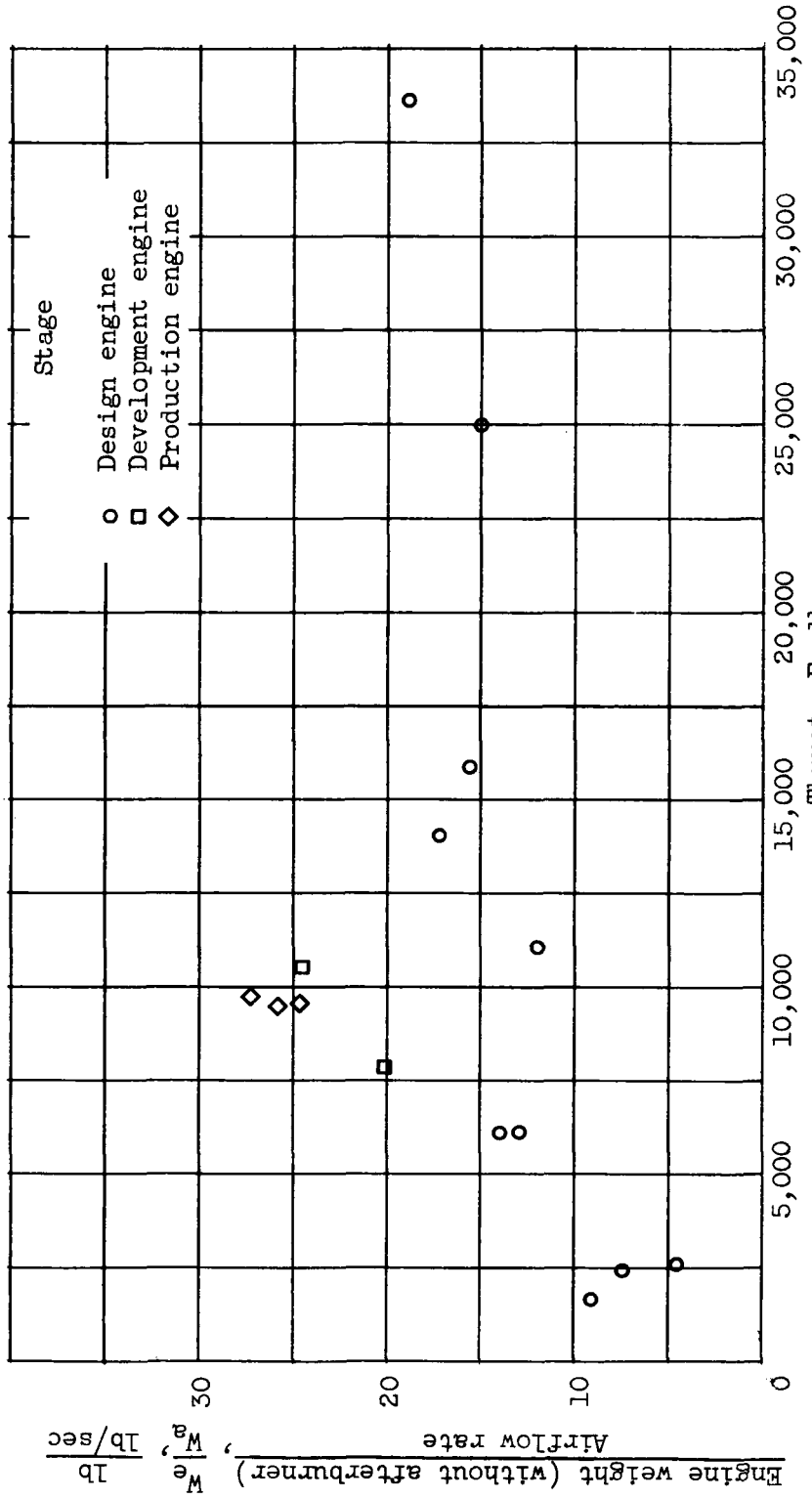

Figure 17. - Variation of ratio of nonafterburner engine weight to airflow rate with thrust at sea-level static conditions.

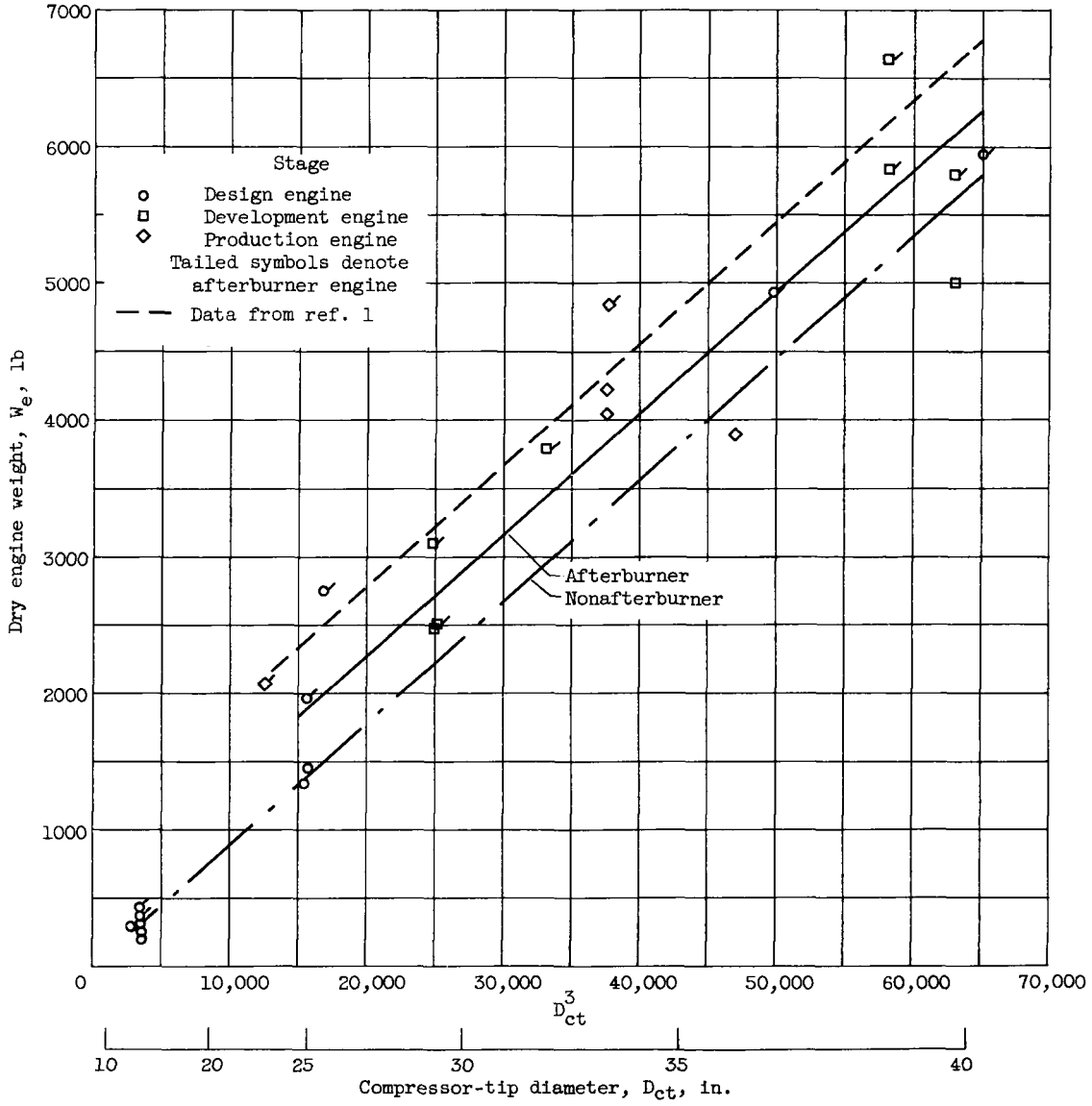

Figure 18. - Variation of engine weight with compressor-tip diameter.

[redacted]

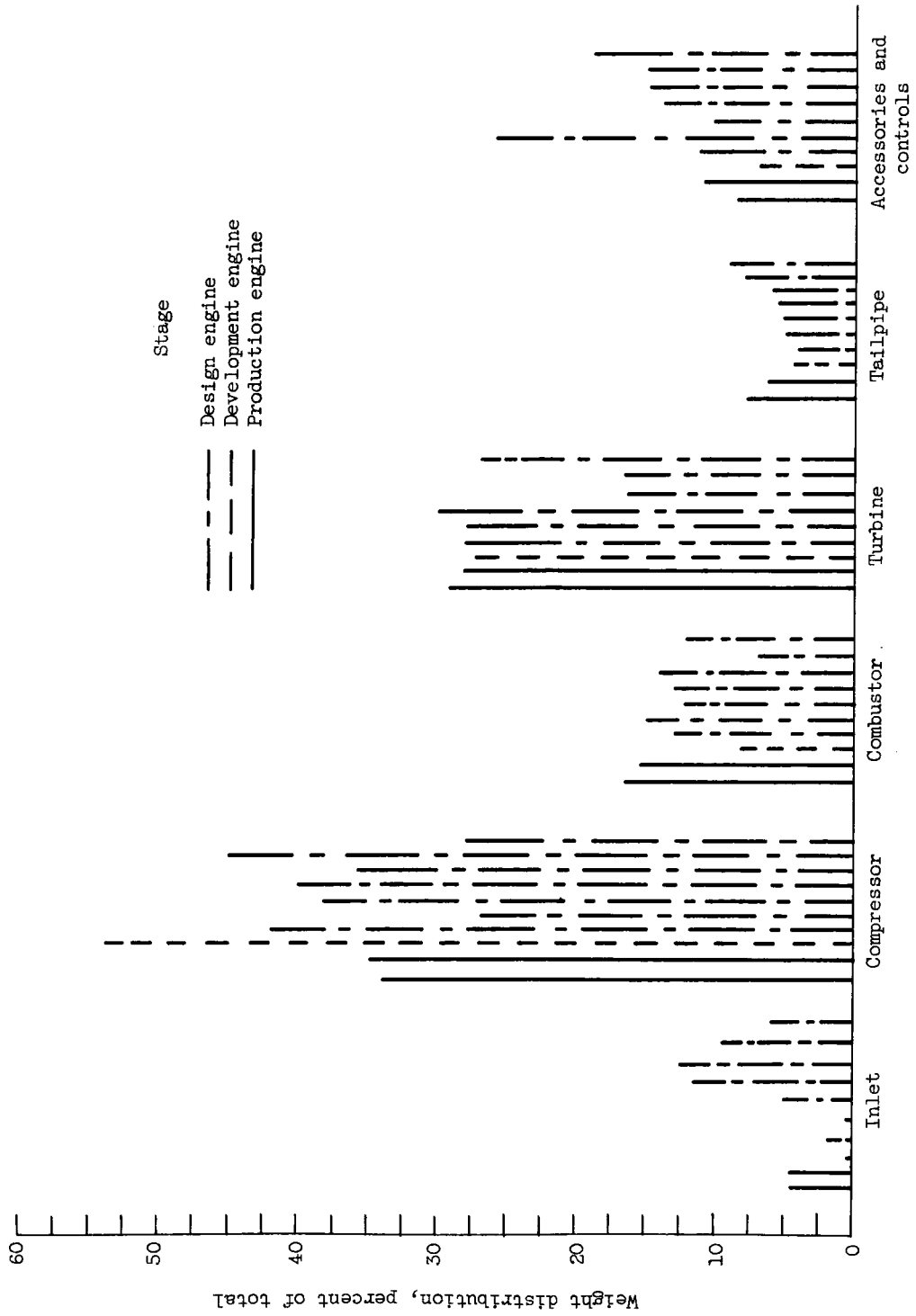

(a) Nonafterburner engines.

Figure 19. - Engine-component weight distribution.

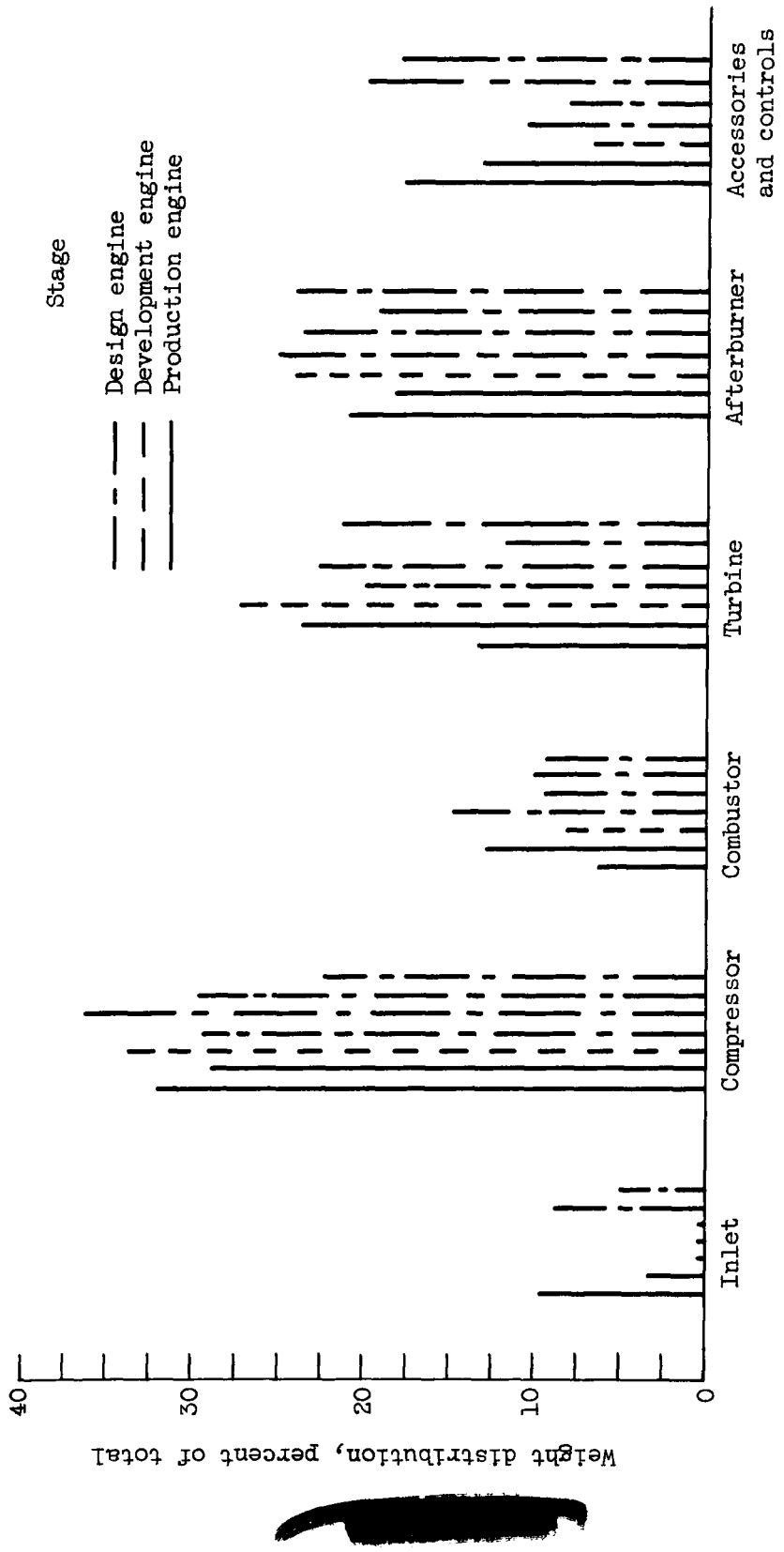

(b) Afterburner engines.

Figure 19. - Concluded. Engine-component weight distribution.

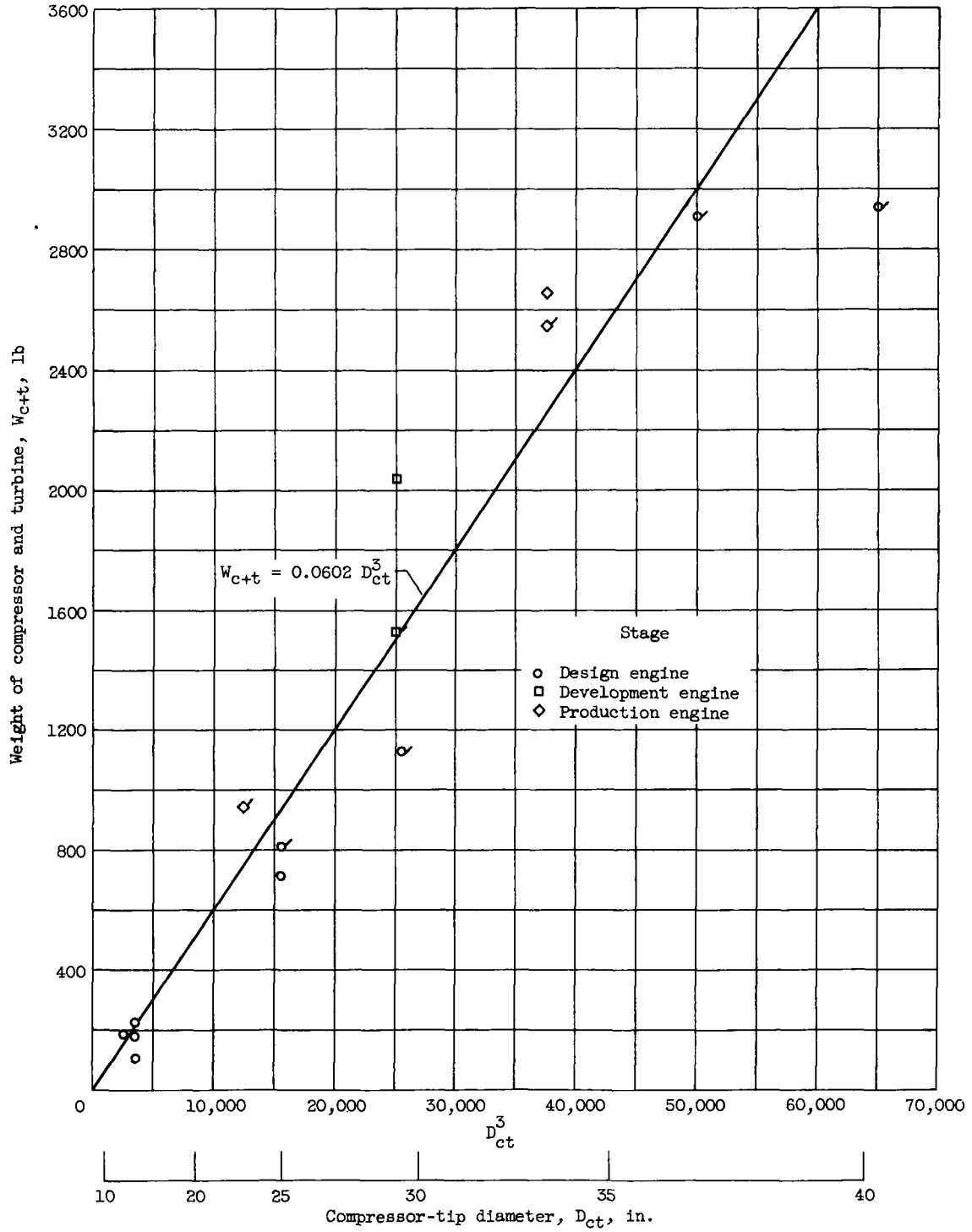

Figure 20. - Variation of combined weight of compressor and turbine with compressor-tip diameter.

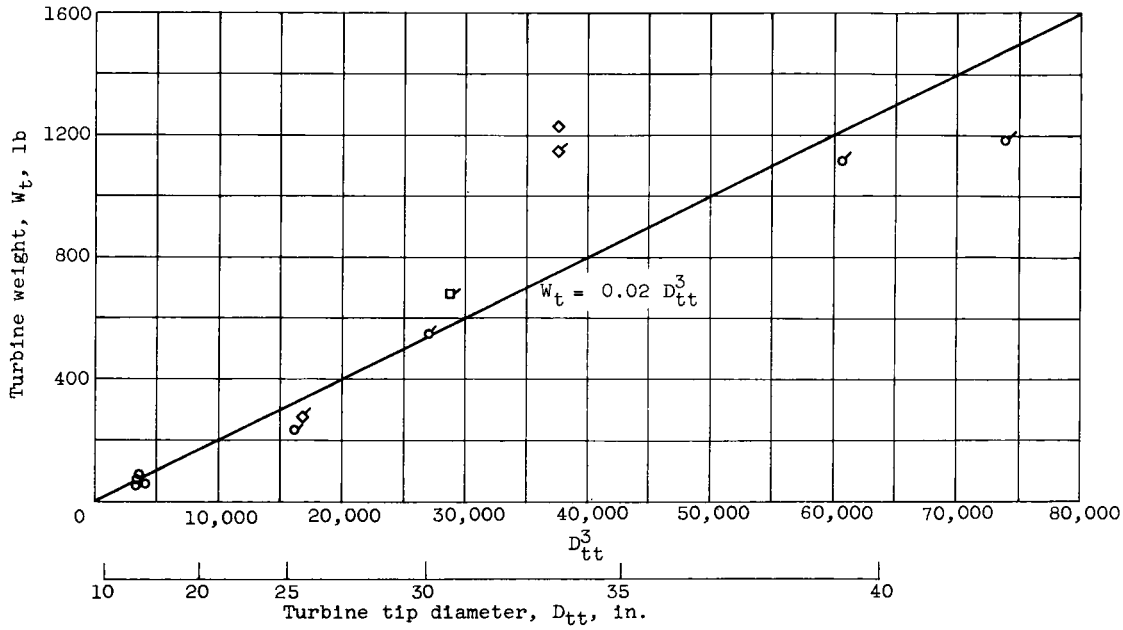

Figure 21. - Variation of turbine weight with turbine-tip diameter.

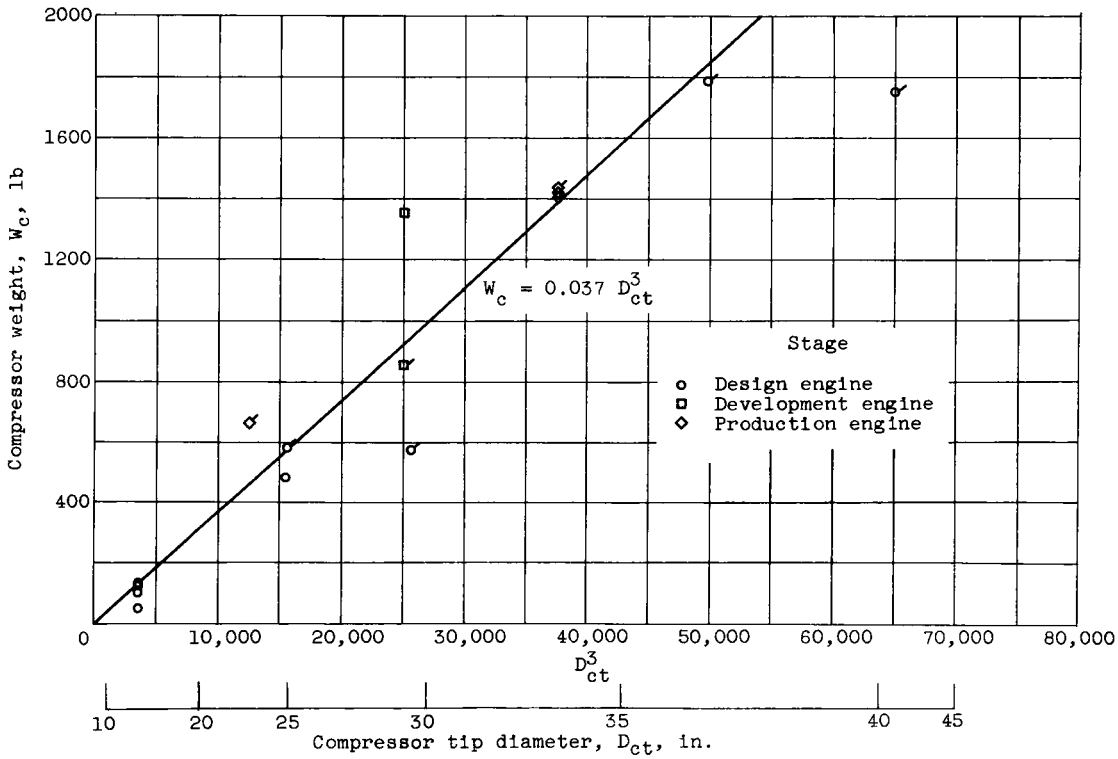

Figure 22. - Variation of compressor weight with compressor-tip diameter.

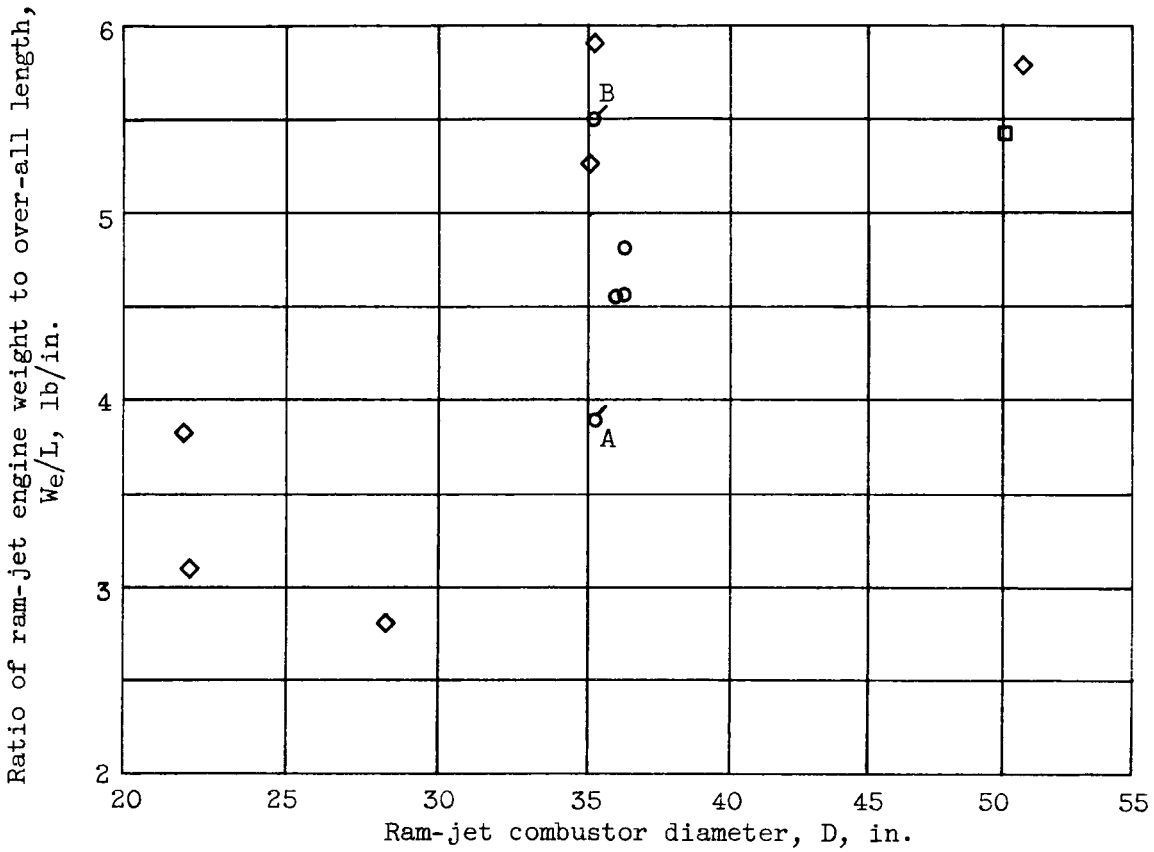

Figure 23. - Effect of combustor diameter on ram-jet weight per foot of length.

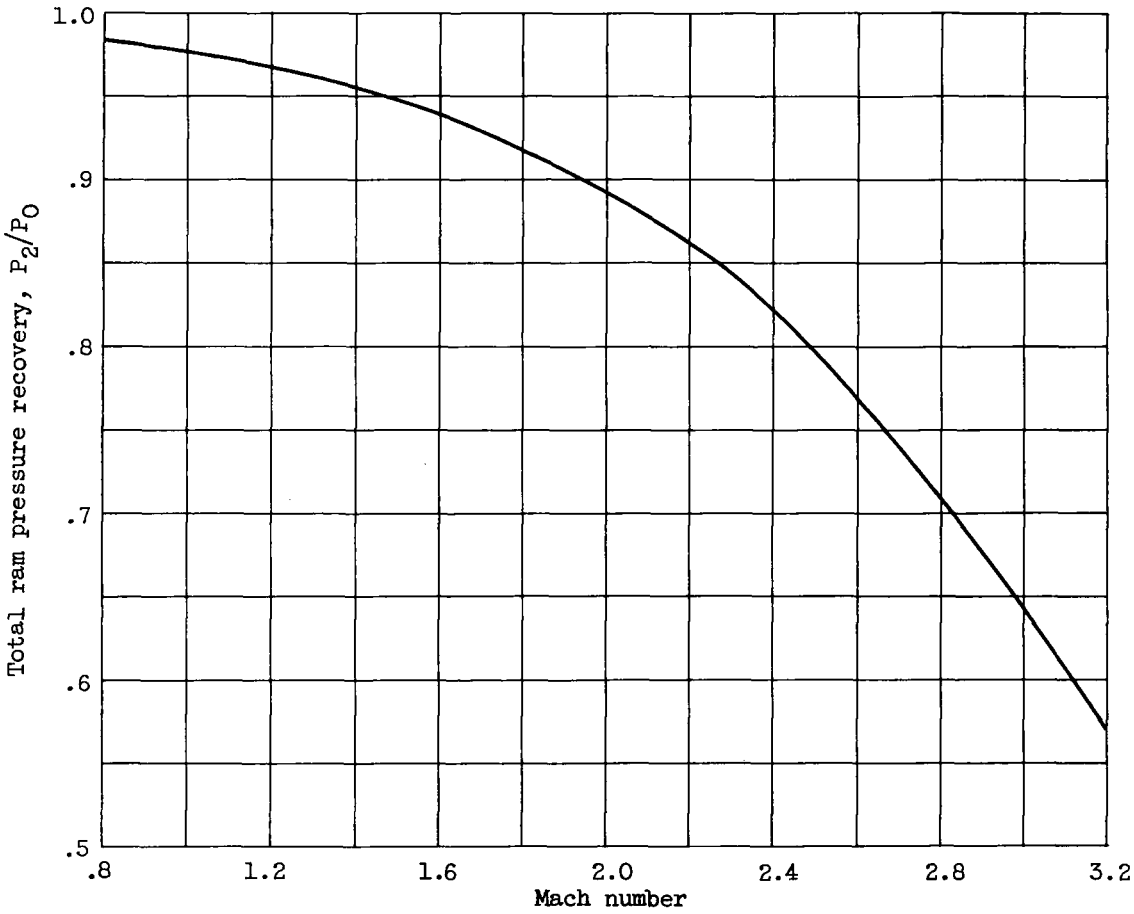

Figure 24. - Total ram pressure recovery used for performance data. Curve based on experimental data from NACA inlet investigations.

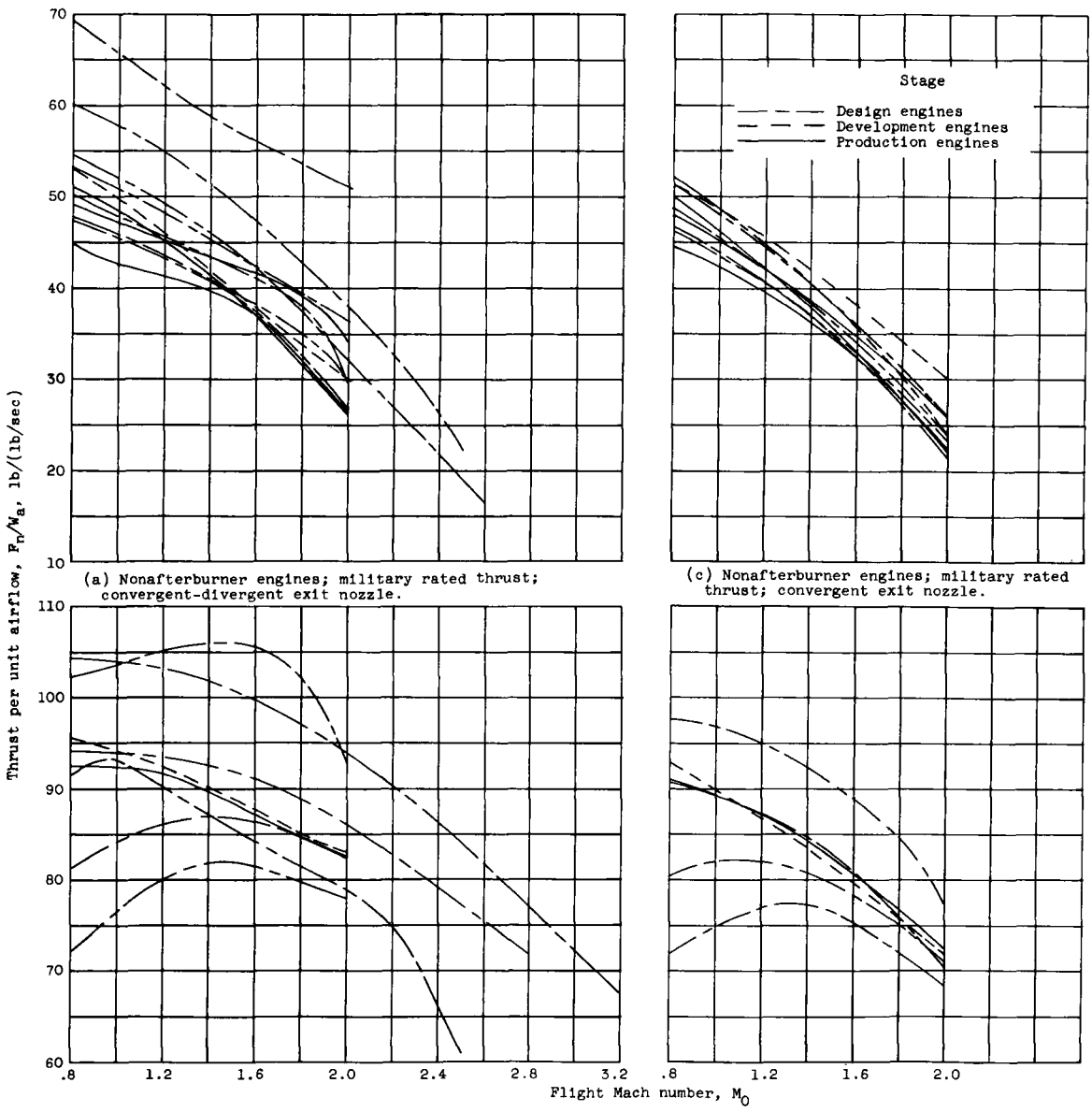

(a) Nonafterburner engines; military rated thrust; convergent-divergent exit nozzle.

(c) Nonafterburner engines; military rated thrust; convergent exit nozzle.

(b) Afterburner engines; maximum rated thrust; convergent-divergent exit nozzle.

(d) Afterburner engines; maximum thrust; convergent exit nozzles.

Figure 25. - Variation of thrust per pound of airflow with flight Mach number. Altitude, 35,000 feet.

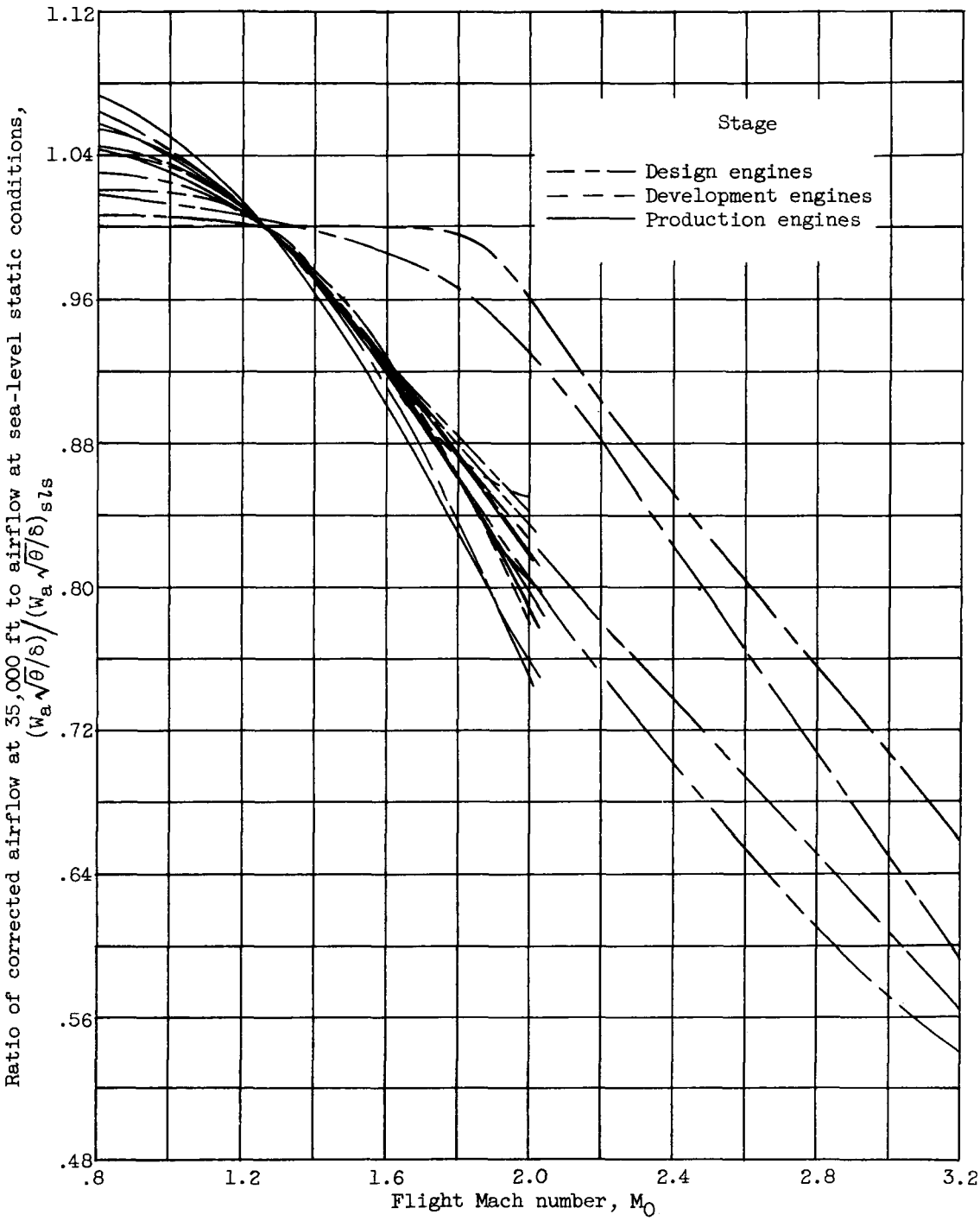

Figure 26. - Variation of corrected airflow with flight Mach number.

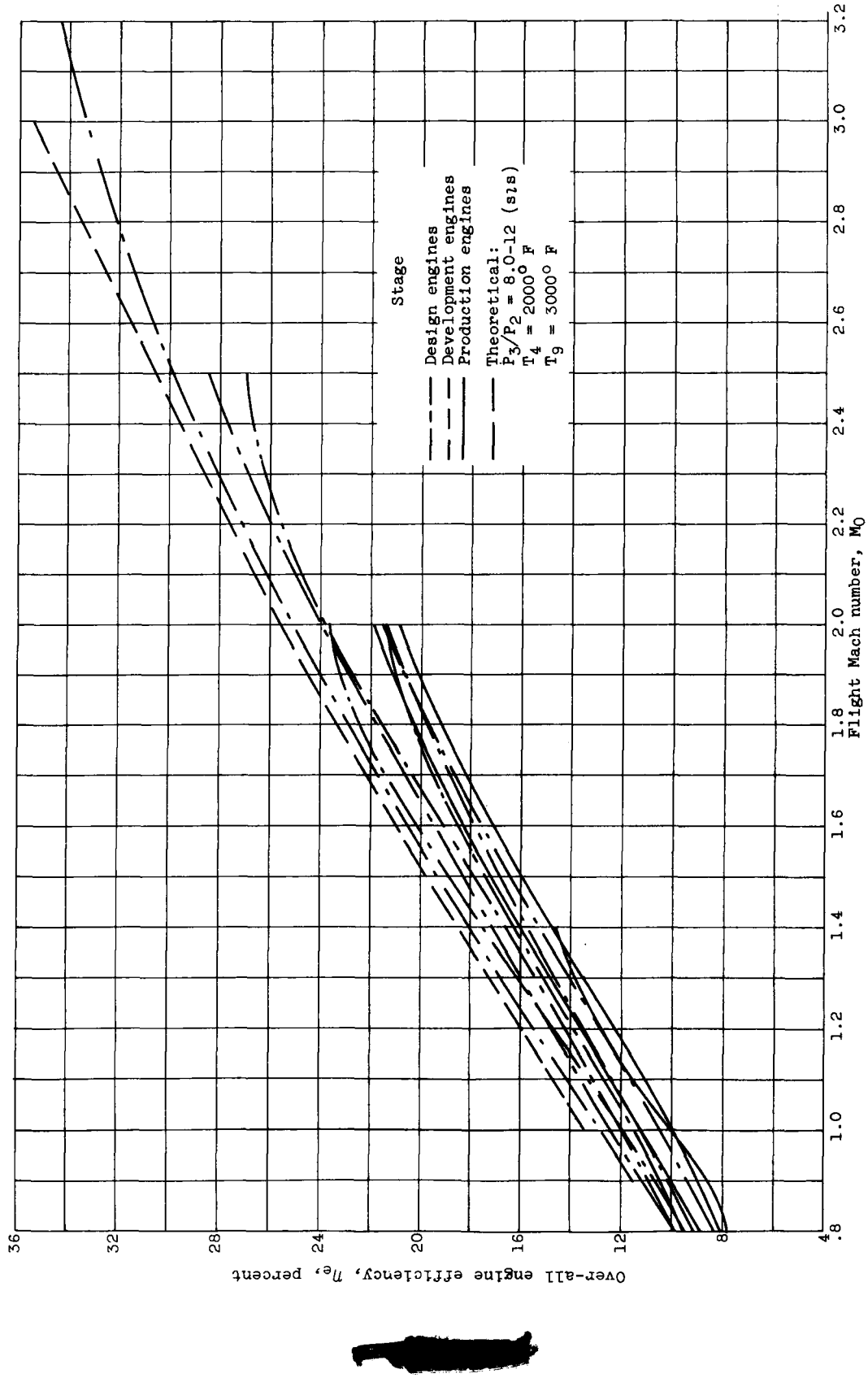

(a) Afterburner engines.

Figure 27. - Effect of flight speed on over-all engine efficiency. Altitude, 35,000 feet.

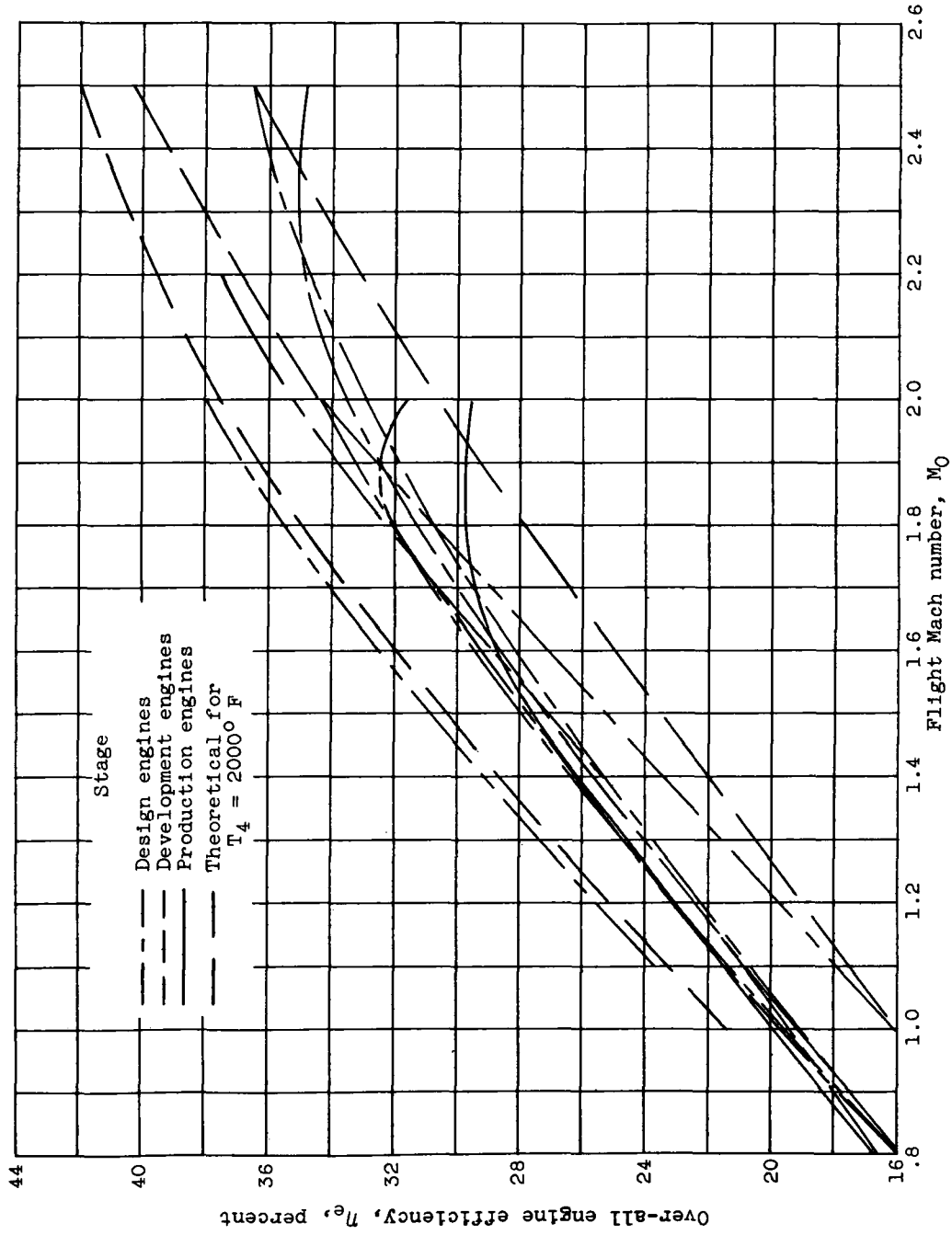

(b) Nonafterburner engines.

Figure 27. - Concluded. Effect of flight speed on over-all engine efficiency. Altitude, 35,000 feet.

4339

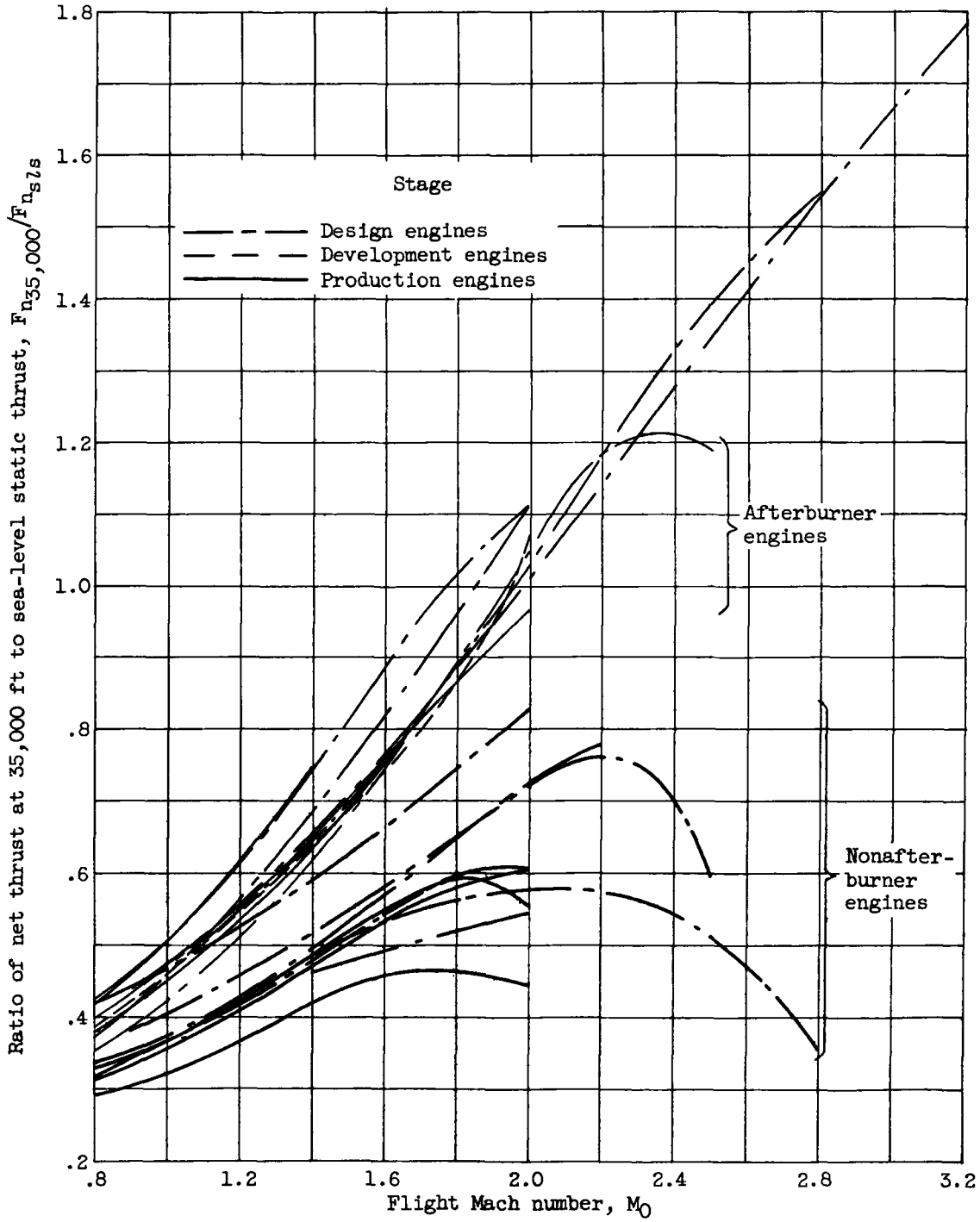

Figure 28. - Variation of thrust ratio with Mach number.

[redacted]

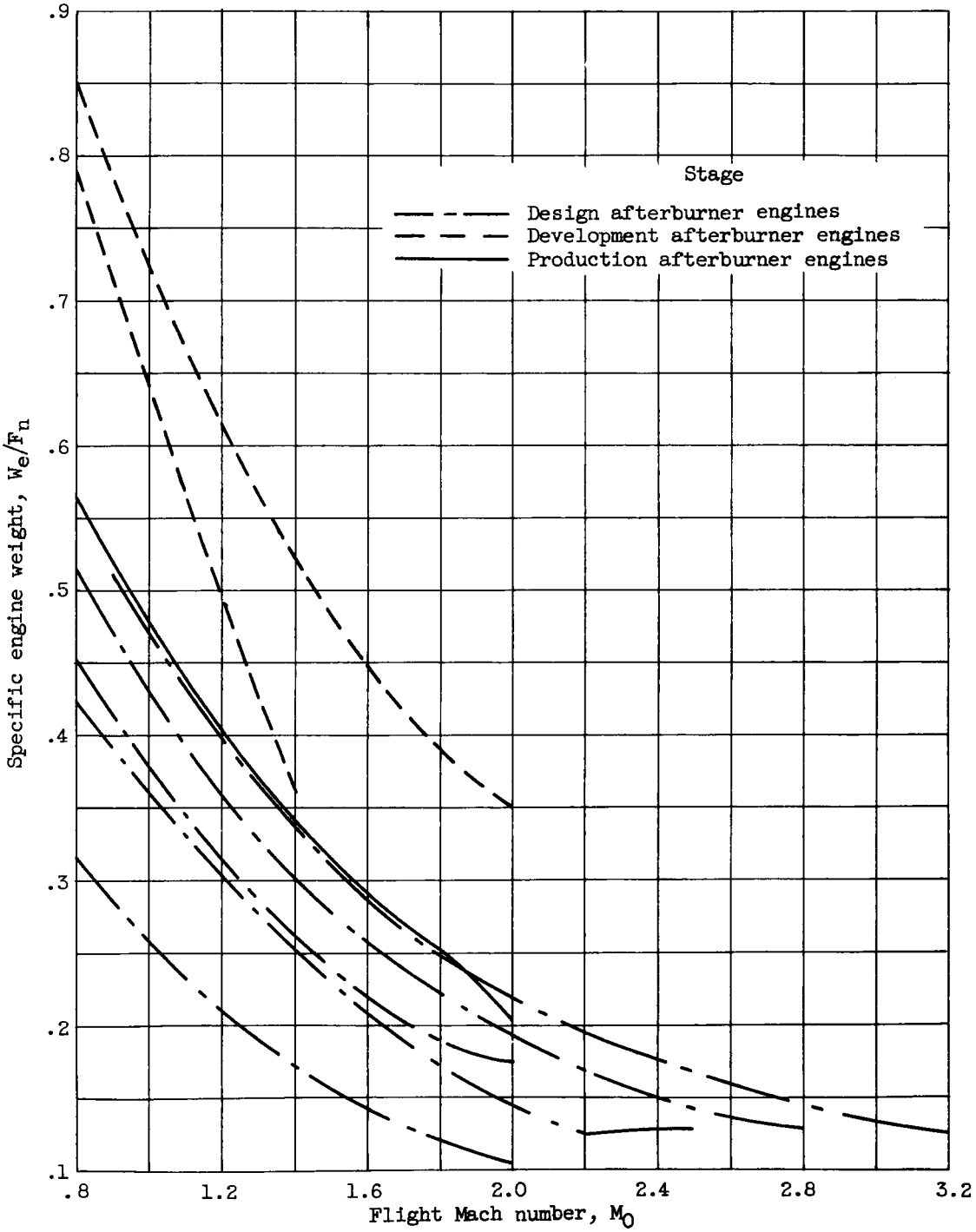

(a) Afterburner engines.

Figure 29. - Effect of flight speed on specific turbine weight. Altitude, 35,000 feet.

[redacted]

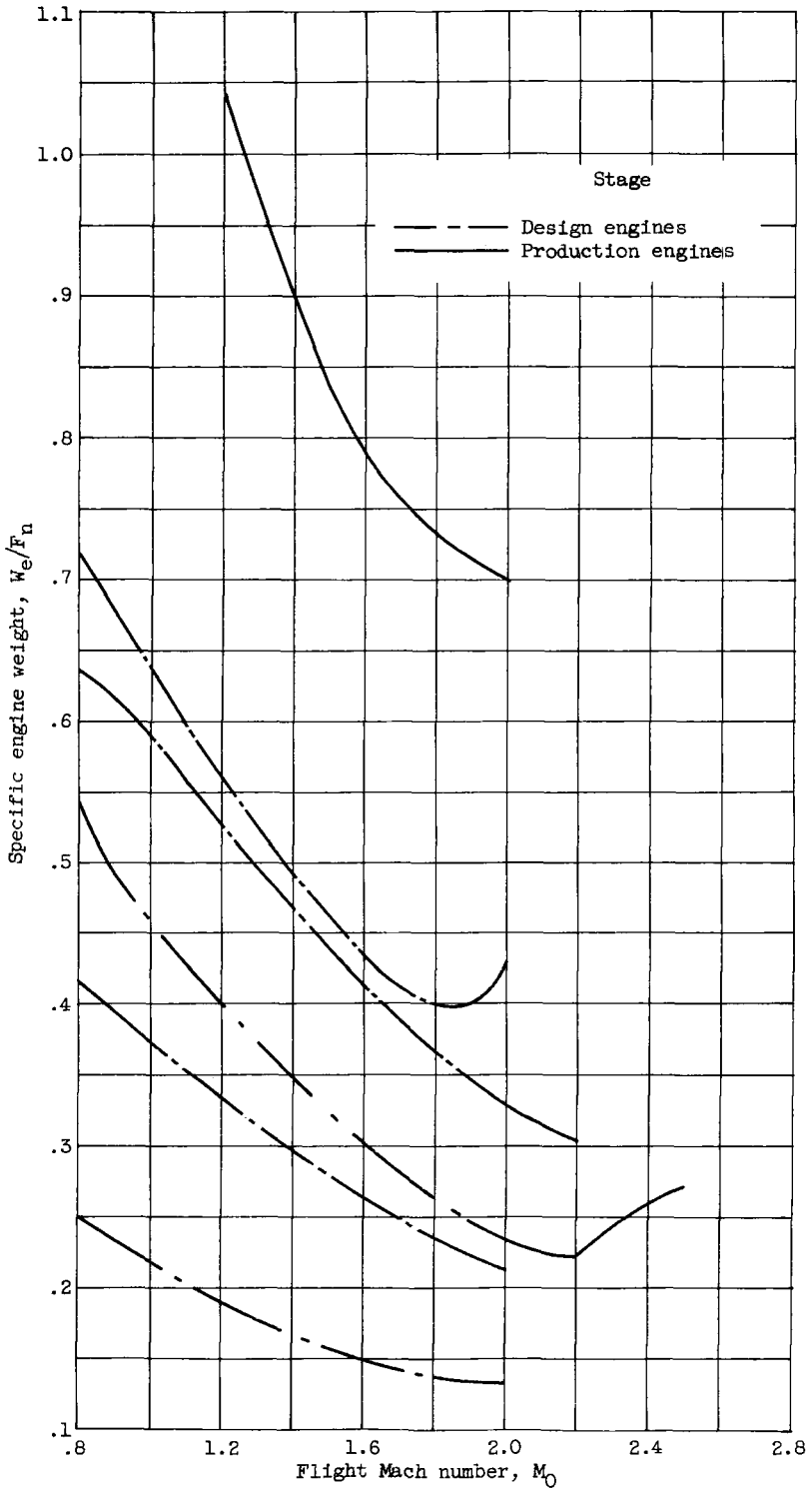

(b) Nonafterburner engines.

Figure 29. - Concluded. Effect of flight speed on specific engine weight. Altitude, 35,000 feet.

[redacted]

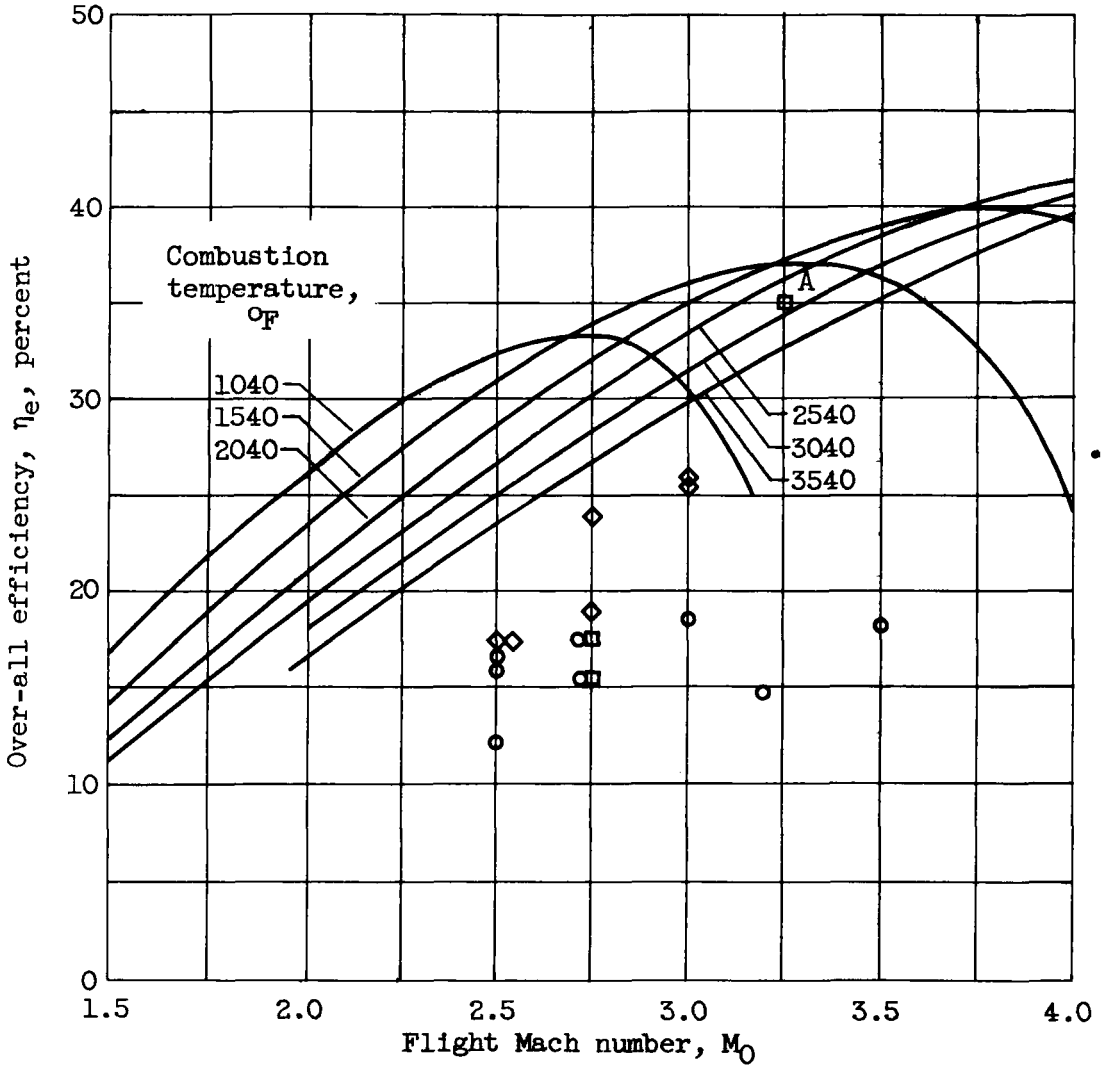

Figure 30. - Ram-jet efficiency as a function of flight Mach number and combustion temperature. Ram-jet performance: two-wedge inlet; $M_2 = 0.175$; $\eta_t = 0.90$; JP-4 fuel; $C_v = 0.96$.

[redacted]

4339

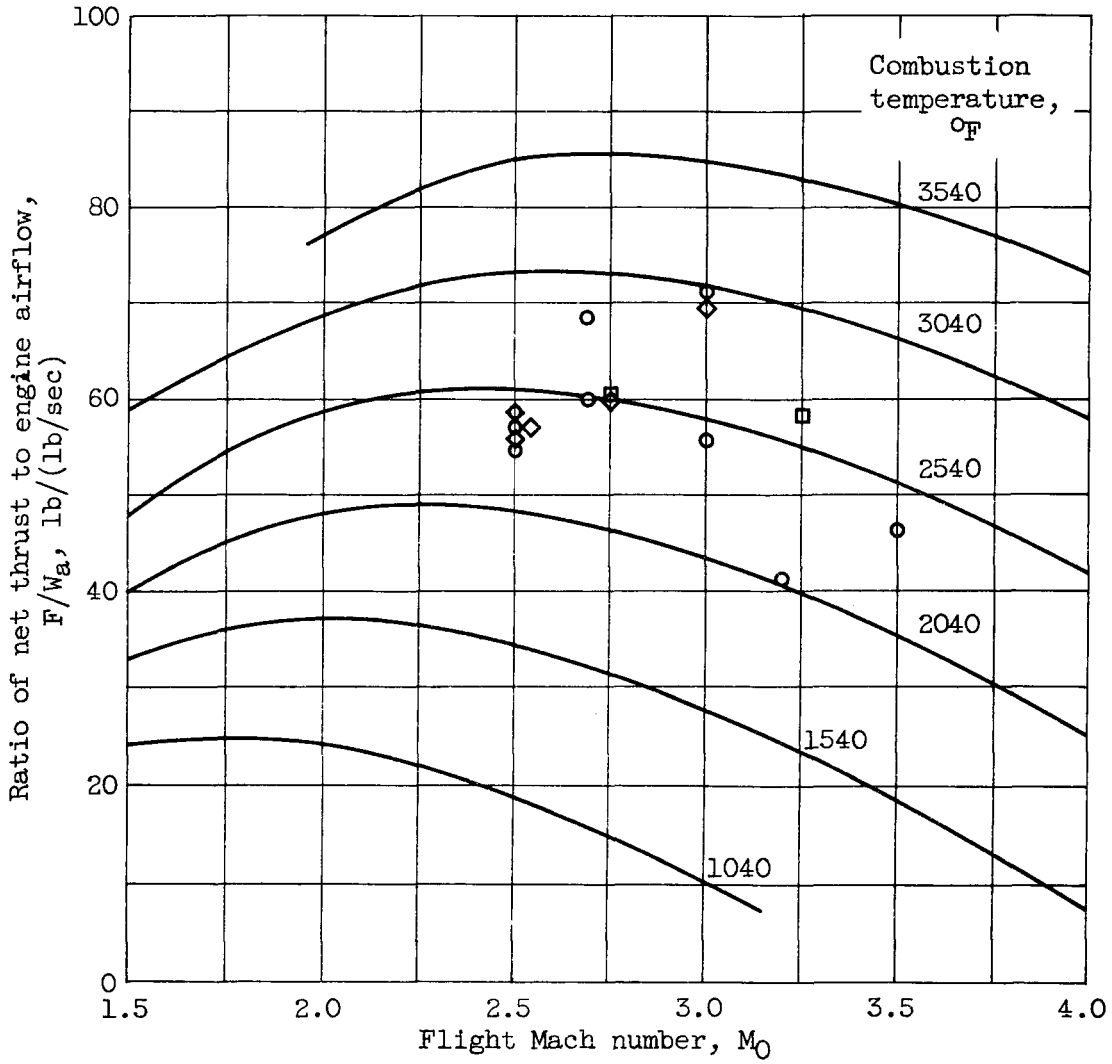

Figure 31. - Variation of ratio of thrust to airflow with flight Mach number. Ram-jet performance: No external drag; two-wedge inlet; combustion-chamber inlet Mach number, 0.175; combustion efficiency, 0.90; JP-4 fuel; exhaust-nozzle velocity coefficient, 0.96.

[redacted]

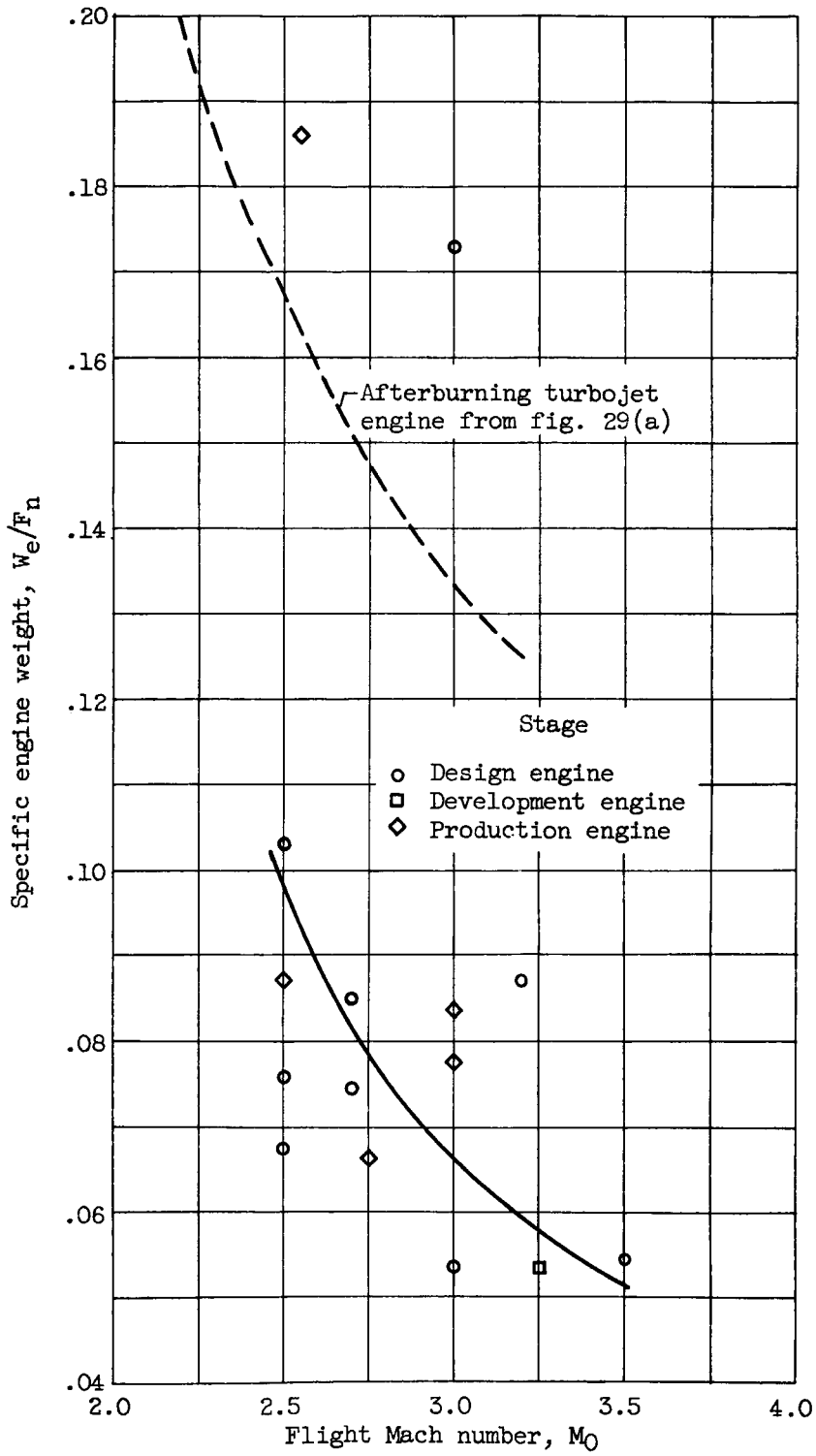

Figure 32. - Effect of flight Mach number on ram-jet specific engine weight; altitude, 35,000 feet.